Influence of Pseudo-Jahn-Teller Activity on the Singlet-Triplet Gap of Azaphenalenes

Atreyee Majumdar, Komal Jindal, Surajit Das, and Raghunathan Ramakrishnan, and Tata Institute of Fundamental Research, Hyderabad 500046, India

(Dated: 8 October 2024)

We analyze the possibility of symmetry-lowering induced by pseudo-Jahn-Teller interactions in six previously studied azaphenalenes that are known to have their first excited singlet state (S_1) lower in energy than the triplet state (T₁). The primary aim of this study is to explore whether Hund's rule violation is observed in these molecules when their structures are distorted from C_{2v} or D_{3h} point group symmetries by vibronic coupling. Along two interatomic distances connecting these point groups to their subgroups $C_{\rm s}$ or $C_{3\rm h}$, we relaxed the other internal degrees of freedom and calculated two-dimensional potential energy subsurfaces. The many-body perturbation theory (MP2) suggests that the high-symmetry structures are the energy minima for all six systems. However, single-point energy calculations using the coupled-cluster method (CCSD(T)) indicate symmetry lowering in four cases. The singlet-triplet energy gap plotted on the potential energy surface also shows variations when deviating from high-symmetry structures. A full geometry optimization at the CCSD(T) level with the cc-pVTZ basis set reveals that the D_{3h} structure of cyclazine (1AP) is a saddle point, connecting two equivalent minima of C_{3h} symmetry undergoing rapid automerization. The combined effects of symmetry lowering and high-level corrections result in a nearly zero singlet-triplet gap for the C_{3h} structure of cyclazine. Azaphenalenes containing nitrogen atoms at electron-deficient sites—2AP, 3AP, and 4AP—exhibit more pronounced in-plane structural distortion; the effect is captured by the long-range exchange-interaction corrected DFT method, ω B97XD. Excited state calculations of these systems indicate that in their low-symmetry energy minima, T_1 is indeed lower in energy than S_1 , upholding the validity of Hund's rule. Jahn-Teller analysis predicts the symmetries of the in-plane distortion vibrational modes as $A_2':D_{3h}\to C_{3h}$ or $B_2:C_{2v}\to C_s$ agreeing with the vibrational frequencies of the saddle-points.

Keywords: Azaphenalenes, Jahn–Teller effect, vibronic coupling, excited states, singlet-triplet energy gap, Hund's rule

I. INTRODUCTION

Azaphenalene (1AP in FIG. 1), also known as monoazaphenalene, cycl[3.3.3]azine, or cyclazine, and its polyaza analogues, wherein nitrogen (N) atoms replace the peripheral CH groups, display a potential to violate the Hund's rule¹—their first excited singlet state, S_1 , is suggested to be lower in energy than the triplet counterpart, T_1^{2-16} . Three-fold symmetric $1AP^{17}$ and heptazine (7AP)^{18,19} were among the first APs synthesized, followed by the two-fold symmetric, pentazine (5AP), along with a few other asymmetric APs²⁰; see FIG. 1 for the structures of 5AP and 7AP. Gimarc²¹ ascribed the stability of 7AP to the substitution of the CH moiety by N at the sites of 1AP with significant densities of the highest occupied molecular orbital (HOMO), as shown in FIG. 1. This topological charge stabilization effect 21 rationalized the synthesis of another threefold symmetric AP²². A similar effect diminishes antiaromaticity through double-bond localizations in substituted indacene²³ and pentalene^{24–26} that, along with APs, are among the too few molecular cores identified so far to exhibit negative STGs. A search for other examples in the chemical space of small organic molecules showed no evidence of STG inversion²⁷.

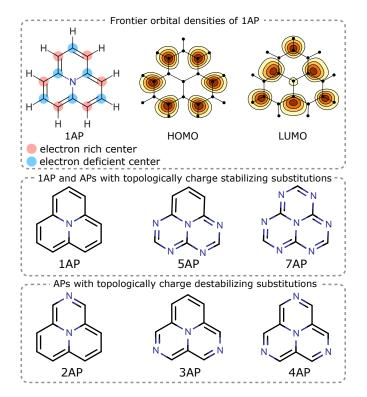


FIG. 1. Representation of APs explored in the present study, and density contours of the frontier MOs of 1AP.

a) Electronic mail: ramakrishnan@tifrh.res.in

Leupin et al. were the first to suggest the likelihood of a negative S_1-T_1 gap (STG) in 7AP²⁸. Its photochemistry exhibits delayed fluorescence, characteristic of a small, negative STG³. Further, fluorescence measurements suggested an STG of -0.011 eV for a substituted 7AP⁵. Finite-temperature Wigner phase space sampling of two experimentally studied derivatives of 7AP has revealed the out-of-plane distortion of the equilibrium geometry of the S_1 state to play a role in the downhill reverse-intersystem-crossing (rISC) mechanism²⁹. More recently, an absorption spectrum confirmed the STG of 5AP in argon matrix to be -0.047 ± 0.007 eV³⁰ aligning with independent measurements on dialkylaminesubstituted 5AP³¹. Inverted STG promises the scope for designing the next generation organic light emitting diodes (OLEDs), with efficiencies not limited by spin statistics 5,6,11.

In this study, we investigate structural preferences exhibited by APs shown in FIG. 1 and explore how symmetry lowering, driven by second-order Jahn-Teller (SOJT) interactions, impacts their STGs. We first focus on 1AP, 5AP, and 7AP for which Loos et al. 13 performed detailed calculations of STGs and provided the theoretical best estimates (TBEs) as -0.131 eV, -0.119 eV, and -0.219eV, respectively. We also examine the three APs—2AP, 3AP, and 4AP—containing N at electron-deficient sites of 1AP (see FIG. 1). Though these molecules lack experimental measurements, they are of theoretical interest. Loos et al. ¹³ also reported TBEs of their STGs as -0.071eV (2AP), -0.042 eV (3AP), and -0.029 eV (4AP). In the calculations of TBEs¹³, geometries were determined using the accurate method, CCSD(T), by enforcing the maximum symmetry point group for each composition: D_{3h} for 1AP, 4AP, and 7AP; C_{2v} for 2AP, 5AP, and 3AP. For this purpose, MP2 minimum energy structures verified through frequency analysis were selected as initial geometries for subsequent geometry refinement at the CCSD(T) level of theory. Other studies have also applied geometries determined with MP2^{2,9} or using DFT methods such as B3LYP⁸ and ω B97X-D¹⁵.

Elaborate analysis using wavefunction methods and large basis sets have scrutinized the validity of Hund's rule violation by APs³². Other works have shown the limitations of time-dependent DFT (TD-DFT) with functionals lacking a correlation term at the MP2 level to predict negative STGs of APs^{8,9,13,33,34}. The nature of the potential energy surface (PES) of APs and its impact on their STGs has received less attention. For 1AP, early calculations²⁸ suggested a C_{3h} structure with alternating bond lengths, contrasting the D_{3h} structure typical of an aromatic system. However, calculations using $\mathrm{DFT^2}$ and $\mathrm{MP2^3}$ methods predicted a symmetric structure, which has since been widely adopted. It is interesting to note that MP2 predicts a planar, D_{3h} structure for phosphaphenalene containing a phosphorous atom in the triangulene core of 1AP instead of N, while the B97-3C-DFT method indicates a distortion of the geometry towards the pyramidal, C_{3v} structure⁷. Although more

accurate calculations of 1AP have been performed using the CCSD(T) method¹³, vibrational analysis at this level remains challenging when using a triple-zeta quality basis set. Additionally, determining an initial geometry for CCSD(T)-level explorations to assess the relative stability of iso-energetic structures is non-trivial, as approximate methods exclusively prefer symmetric structures. Consequently, the true nature of the PES of 1AP remains elusive.

Given the complexity of the problem, an out-of-the-box approach is necessary to investigate the structural preferences of APs. We examine symmetry-lowering in APs from the highest point group symmetry, permitted by their composition and connectivities, to their maximum-order subgroups. To probe for symmetry lowering and the variation of STG on a lower-dimensional potential energy surface, we conducted a diagnostic procedure, which we denote as Jahn-Teller-Hund's (JTH) diagnostics. We determine the PES of APs using the CCSD(T) method, which is more accurate than MP2, to probe for changes in qualitative aspects of the PES due to electron correlation effects. Further, we inspect the variation of the STG across the PES.

II. COMPUTATIONAL DETAILS

For all APs shown in FIG. 1, we performed full geometry optimizations by constraining the point group symmetries and relaxing the internal coordinates defined through the Z-matrix representation; see SI for the definitions of Z-matrices. The main goal of our study is to verify whether the high-symmetric structures of the APs shown in FIG. 1 correspond to minima on the PES. Hence, we have separately performed full geometry optimizations at the CCSD(T)/cc-pVTZ level for high-symmetric and low-symmetric structures. For all six APs, the high-symmetric structures have been reported in an earlier study 13 . In cases where the high-symmetric structures are saddle points on the PES, they cannot be used as a starting point to determine the low-symmetric structures because, at the saddle points, the forces on the atoms are zero. Hence, we select initial geometries of low-symmetric structures identified in JTH diagnostic analysis performed with the smaller basis set cc-pVDZ.

As the first step of JTH diagnostics, MP2/cc-pVDZ-level constrained geometry optimizations were performed using Z-matrices by fixing two interatomic distances (r_1 and r_2 in FIGs. 2 and 3) at $r_1 \in [1.30\,\text{Å}, 1.50\,\text{Å}]$ and $r_2 \in [1.30\,\text{Å}, r_1]$, in steps of 0.01 Å. For plotting the resulting two-dimensional PES, discrete points were interpolated using cubic functions as implemented in the matplotlib module in Python. To probe the effect of electron correlation and the variation of STG across the PES, single-point calculations of the ground and excited state energies were calculated using the CCSD(T) and ADC(2) methods, respectively, in combination with the cc-pVDZ basis set.

Structures corresponding to the lowest CCSD(T)/ccpVDZ energy in the JTH diagnostic plots were selected as initial structures for full optimization. For 1AP, 2AP, 3AP, and 4AP, these structures correspond to the low-symmetry point groups $C_{3\mathrm{h}}$, C_{s} , C_{s} , and $C_{3\mathrm{h}}$, respectively, indicating the likelihood of symmetry lowering. For the same systems, minimum energy structures along the $r_1=r_2$ line were selected as initial geometries for full optimization of high-symmetry point groups. For 5AP and 7AP, CCSD(T)/cc-pVDZ energies did not indicate symmetry lowering. Hence, geometry optimizations were performed only for the high-symmetry structures ($C_{2\mathrm{v}}$ and $D_{3\mathrm{h}}$ for 5AP and 7AP, respectively).

For all molecules, equilibrium geometries were also determined using the DFT methods, B3LYP³⁵ and ω B97X-D³⁶, along with the wavefunction methods MP2, CCSD and CCSD(T) in combination with the cc-pVTZ basis set. Harmonic frequency analyses were performed with DFT and MP2 methods to confirm if the structures were minima or saddle points on their respective potential energy surfaces. DFT-level geometry optimizations were conducted using Gaussian (version 16 C.01)³⁷. MP2, CCSD, and CCSD(T) geometry optimizations were performed using Molpro (version 2015.1)³⁸. For determining STGs, S₁ and T₁ energies were calculated using the excited states method, ADC(2), employing the resolutionof-identity (RI) approximation^{39,40} as implemented in QChem (version 6.0.2)⁴¹ at the cc-pVTZ basis set. All calculations based on the correlated wavefunction methods MP2, CCSD, CCSD(T), and ADC(2) were performed with the frozen-core approximation. Complete basis set (CBS) extrapolation was performed using the two-point formula that uses CCSD(T) energies determined with the cc-pVTZ and cc-pVQZ basis sets. Hartree-Fock (HF) energy from the cc-pVQZ basis set is taken as the reference for the CBS estimate, while the correlation energy is extrapolated using the formula $E_{\rm corr}^n = E_{\rm corr}^{\rm CBS} + \alpha n^{-3}$, where n is the cardinal number of the basis set. Normal mode and nucleus-independent chemical shifts (NICS)⁴² analyses were conducted with the $\omega B97X-D3$ method and the cc-pVTZ basis set using Orca (version 5.0.4)^{43,44}. For both analyses, minimum energy geometries were calculated using $\omega B97X-D/cc-pVTZ$ were utilized. The NICS value was calculated as the negative of the magnetic shielding of a ghost atom placed 1 Å above the centroid of each ring to determine isotropic and outof-plane NICS, denoted NICS(1)_{iso} and NICS(1)_{zz}, respectively. In all calculations performed with Orca, we used the resolution-of-identity (RI) approximation^{39,40} and the 'chain-of-spheres' (COS) algorithm for exchange integrals (RIJCOSX).

III. RESULTS AND DISCUSSION

A. Jahn-Teller-Hund diagnostic plots

We begin our analysis with the two-dimensional PESs of 1AP, 5AP, and 7AP, obtained through constrained geometry optimizations by fixing two interatomic distances related by two-fold rotation, see FIG. 2. Using the Z-matrix representation, we constrained the molecules to be in the $C_{3\rm h}$ (for 1AP and 7AP) and $C_{\rm s}$ (for 5AP) subspaces. MP2-level ground state electronic energy surface shows prominent single-well behavior for all three systems with 1AP, 5AP, and 7AP preferring $D_{3\rm h}$, $C_{2\rm v}$, and $D_{3\rm h}$ structures with $r_1=r_2=1.42$ Å, 1.41 Å, and 1.40 Å, respectively. Subsequent MP2/cc-pVTZ-level geometry optimizations and harmonic vibrational frequency analysis described these symmetric structures as minima on the PESs.

CCSD(T) energies calculated in a single-point fashion identify two equivalent minima of 1AP corresponding to C_{3h} symmetry at $\{r_1 = 1.44 \text{ Å}, r_2 = 1.41 \text{ Å}\}$ and $\{r_1 = 1.41 \text{ Å}, r_2 = 1.44 \text{ Å}\}$, see FIG. 2. The D_{3h} structure predicted as a minimum by MP2 shows characteristics of a saddle point at the CCSD(T)-level. It is important to note that the transition state structure is more sensitive to electron correlation effects and MP2 has a tendency to overestimate the importance of double excitations for transition state structures⁴⁵. Another classic example is cyclobutyne, which MP2 predicts as a minimum but is found to be a first-order saddle point by the more accurate CCSD(T) and CCSDT methods⁴⁶. As the HOMO-LUMO gap increases upon substitution of N in the electron-rich sites of 1APwith values of about 6/8/10 eV for 1AP/5AP/7AP, respectively—electron correlation effects become less relevant. Hence, the PESs of 5AP and 7AP remain similar at both MP2 and CCSD(T) levels. PES plots calculated with the DFT methods, B3LYP and ω B97X-D, are on display in Figure S1 in the Supplementary Information (SI). Both methods forecast single-well type PES for 1AP, 5AP, and 7AP.

In general, for probing the inverted nature of STGs of APs, correlated excited state methods such as ADC(2) or CC2 have provided good estimates^{9,13}. For ten APs, the mean unsigned errors in the STGs predicted by ADC(2) and CC2 were reported to be 0.033 and 0.037 eV¹³. However, EOM-CCSD with similar computational cost as ADC(2) and CC2 has been shown to have a slightly larger error of 0.081 eV^{13} . For 7AP, the similarity-transformed EOM-CCSD method has predicted a too-negative STG of -0.66 eV^8 , compared to its TBE value of -0.219 eV^{13} . STGs calculated on the PES with the ADC(2) method and cc-pVDZ basis set identifies regions where S_1 is lower in energy than T_1 , see FIG. 2. For all three molecules, symmetric structures exhibit inverted STG. Individual plots of S_1 and T_1 relative to S_0 are on display in Figure S2, where one notices that the S_1 energy drops more rapidly when deviating from the diag-

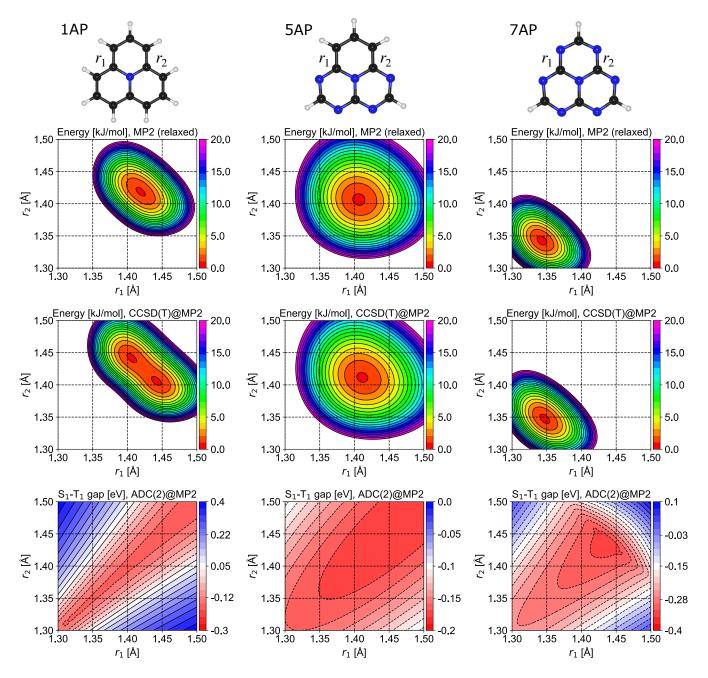


FIG. 2. Contour plots of two-dimensional potential energy surfaces of the ground state and corresponding S_1 - T_1 gaps for 1AP, 5AP, and 7AP. MP2 (relaxed) indicates that each point on the surface was calculated through constrained geometry optimization at the MP2-level for fixed values of $r_1 \in [1.30\,\text{Å}, 1.50\,\text{Å}]$ and $r_2 \in [1.30\,\text{Å}, r_1]$, in steps of 0.01 Å. Discrete points were interpolated as a surface using cubic functions. The point group symmetries were constrained to C_{3h} for 1AP and 7AP, and C_{5} for 5AP; along $r_1 = r_2$, the symmetries are D_{3h} and C_{2v} , respectively. CCSD(T)@MP2 indicates the ground state energy, while ADC(2)@MP2 indicates S_1 - T_1 gap calculated on geometries optimized with MP2 at each point. The ground state energy (in kJ/mol) and the S_1 - T_1 gap (in eV) are color-coded by rainbow and red-to-blue color bars, respectively. Energies above 20 kJ/mol are not shown. In all calculations, cc-pVDZ basis set was used.

onal line (corresponding to symmetric structures) compared to the T_1 energy. Overall, the JTH diagnostics on a low-dimensional PES hints at a symmetry-lowered structure for 1AP with an STG of diminished magnitude while suggesting symmetric structures for 5AP and 7AP with negative STG in agreement with experimental

measurements^{3,30}. For in-plane distortions from the equilibrium geometry along the two interatomic distances, 5AP shows robust Hund's rule violation compared to 7AP. For the latter, FIG. 2 shows regions with positive STG.

FIG 3 presents the JTH diagnostic plots for 2AP, 3AP,

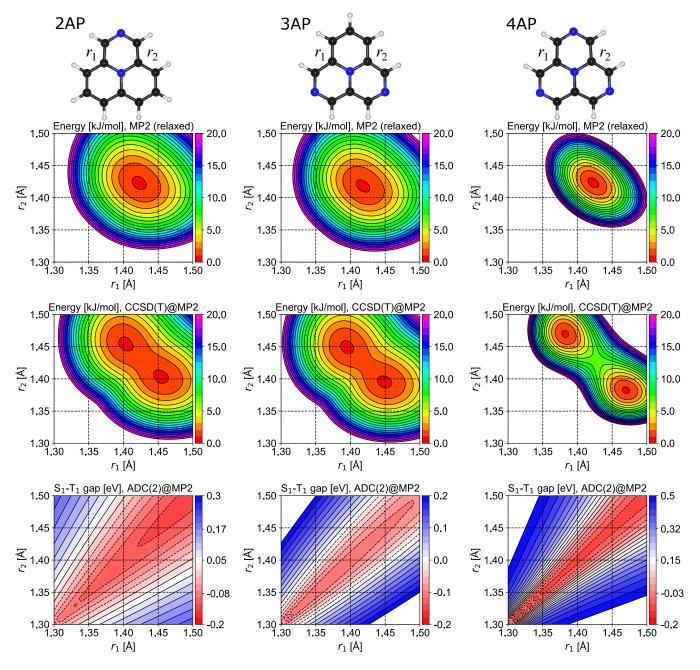


FIG. 3. Contour plots of two-dimensional potential energy surfaces and corresponding S₁-T₁ gaps for 2AP, 3AP, and 4AP. The point group symmetries were constrained to C_{3h} for 4AP, C_{s} for 2AP and 3AP; along $r_{1} = r_{2}$, the symmetries are D_{3h} and C_{2v} , respectively. See the caption of FIG. 2 for further details.

and 4AP. MP2 describes these systems as prominent single-well structures of maximum symmetry (C_{2v} for 2AP and 3AP; D_{3h} for 4AP). MP2/cc-pVTZ geometry refinements and frequency analysis indicated all three symmetric structures to be minima. CCSD(T) energies show a trend contrasting with MP2-level description for all three molecules; in all cases, the high-symmetry structure turns out to be the saddle point connecting low-symmetry structures belonging to the largest subgroup (C_s for 2AP and 3AP; C_{3h} for 4AP). As seen in FIG 3,

the barrier increases with the number of N atoms on charge-destabilizing positions (i.e., LUMO sites of 1AP, see FIG.1). STG plots of all three molecules indicate a profile similar to the one noted for 1AP in FIG. 2. The STG is negative along the $r_1=r_2$ line containing the high-symmetry structures, while for the distorted structures, the plot suggests positive STGs. CCSD(T)/cc-pVTZ geometries were determined using the coordinates of the distorted structures inferred from FIG 3 as the starting point. Subsequent ADC(2)/aug-cc-pVTZ ex-

cited state calculations for 2AP, 3AP, and 4AP resulted in STGs of +0.125 eV, +0.274 eV, and +0.392 eV, respectively (see Table I).

Figure S1 shows the PESs of 2AP, 3AP, and 4AP generated using the DFT methods B3LYP and ω B97X-D. While B3LYP predicts 2AP and 3AP to be single-wells, for 4AP, the method suggests a slight distortion with r_1 and r_2 differing by 0.03 Å. Frequency analysis confirmed the D_{3h} and C_{2v} structures of 2AP and 3AP to be minima at the B3LYP/cc-pVTZ-level, while the symmetric structure of 4AP showed one imaginary frequency $(494i \text{ cm}^{-1})$ A_2'). The long-range corrected DFT method, $\omega B97X$ -D, has been shown to outperform B3LYP in determining minimum energy structures of unusual covalent bond connectivities⁴⁷. For 2AP, ω B97X-D shows a weak distortion in agreement with CCSD(T). At the same time, the method indicates the symmetric geometries of 2AP. 3AP, and 4AP to be saddle points, suggesting the possibility of locating the low-symmetry minima with less expensive DFT modeling (see Figure S1).

B. Geometries and Singlet-Triplet gaps

Table I presents STGs of the selected APs shown in FIG. 1 calculated with ADC(2)/aug-cc-pVTZ using equilibrium geometries determined using the accurate CCSD(T)/cc-pVTZ method. Results based on geometries from other methods are available in the SI (see Tables S1, S2, and S3 for 1AP, 5AP, and 7AP, respectively; Table S4 for 2AP, 3AP, and 4AP). FIG. 4 shows the corresponding equilibrium geometry parameters for both the structures at the CCSD(T)/cc-pVTZ-level. For the D_{3h} structure of 1AP, our ADC(2) value of the STG=-0.142 eV, deviates slightly from the previously obtained TBE of -0.131 eV. Using the basis set limit values of CCSD(T) energies, we find the C_{3h} structure of 1AP to be lower in energy than the D_{3h} structure by only 0.3 kJ/mol.

Had the symmetry lowering been predicted by MP2 or DFT methods but not at the more accurate CCSD(T)-level, then the distortion should be considered artifactual⁴⁸. According to the accurate CCSD(T)-level description, the actual PES of 1AP should be thought of as a very shallow double well permitting strong carbon tunneling⁴⁹, which according to quantum mechanics has to be interpreted as two equivalent C_{3h} structures undergoing rapid automerization. Furthermore, as pointed out earlier by Leupin $et\ al$ the nuclear magnetic resonance (NMR) spectrum of 1AP does not rule out the possibility of a rapid isodynamic equilibrium between two C_{3h} minima²⁸, which aligns with its very low barrier reported in this study.

Rigorous confirmation of the true sign of the STG of 1AP requires consideration of high-level effects such as beyond-ADC(2) treatment of excited state and adiabatic effects along with the symmetry lowering effect. The ADC(2) level STG of the D_{3h} structure of 1AP

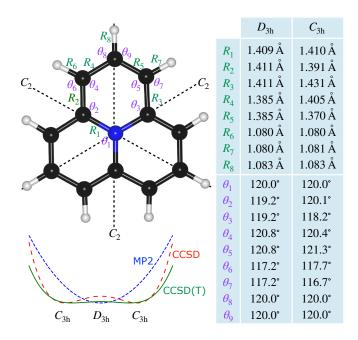


FIG. 4. Equilibrium geometry parameters of 1AP in $D_{3\mathrm{h}}$ (saddle point) and $C_{3\mathrm{h}}$ (minimum) configurations calculated with the CCSD(T)/cc-pVTZ method. Dashed lines show two-fold rotation axes, perpendicular to the principal (three-fold rotation) axis, present in $D_{3\mathrm{h}}$. The schematic PES shows that MP2 describes 1AP as a single-well with the $D_{3\mathrm{h}}$ structure to be the minimum, while CCSD and CCSD(T) suggest a double-well behavior with the lower symmetric $C_{3\mathrm{h}}$ structure as the minimum. At the CCSD(T)-level, the barrier to automerization is vanishingly small, indicating the vibrational ground state's wavefunction is strongly delocalized over the equivalent $C_{3\mathrm{h}}$ minima.

is -0.142 eV determined using vertical excitation energies. Post-ADC(2), high-level corrections can be estimated as +0.009 eV by comparing the STG of the D_{3h} structure from ADC(2) (-0.142 eV) with the TBE (-0.131 eV) from Ref. 13, see Table I. Furthermore, for the D_{3h} structure of 1AP, the vertical STG underestimates the adiabatic transition energy (0-0), which accounts for geometric effects in S_1 and T_1 along with the zero-point vibrational energy, by +0.057 eV at the ADC(2)-level⁹. Using these two corrections, one can estimate the true STG of the D_{3h} structure to be -0.076 eV. Further, for 1AP in the C_{3h} structure, the ADC(2)/augcc-pVTZ value of STG is -0.06 eV shifting the D_{3h} value by +0.082 eV. Hence, one can estimate the 0-0 STG of the C_{3h} structure to be +0.006 eV explaining the small positive experimental STG of $+0.04 \text{ eV}^{28}$. Given the vanishing barrier of 0.3 kJ/mol for automerization, one can expect the wavefunction of the vibrational ground state to span double well broadly. Hence, when the 0-0 STG of 1AP is weighted by the square of this wavefunction, one can expect STG to be vanishingly small, as in the C_{3h} structure.

We performed separate full geometry optimizations for high-symmetry and low-symmetry geometries of 5AP

TABLE I. For the six azaphenalenes shown in FIG. 1, vertical excitation energies of the S_1 and T_1 states with respect to the ground state, S_0 , along with the singlet-triplet gap (S_1-T_1) are given in eV. The excited state energies were calculated using the ADC(2)/aug-cc-pVTZ method using geometries determined with the CCSD(T)/cc-pVTZ method. The barrier for automerization, E^{\ddagger} (in kJ/mol), determined using two-point CBS extrapolation of CCSD(T) energies with cc-pVTZ and cc-pVQZ basis sets, is stated for the symmetric saddle point. Results from other studies are included for comparison; 0-0 indicates adiabatic transition energies accounting for the energy of the vibrational ground state.

System	E^{\ddagger}	S_1	T_1	S_1 - T_1	Source
$\overline{1AP(D_{3h})}$	0.3	0.979	1.121	-0.142	this work
1AP (C_{3h})		1.130	1.190	-0.060	this work
1AP		1.047	1.180	-0.133	$ADC(2)^9$
1AP		0.992	1.068	-0.076	
1AP (D_{3h})		0.979	1.110	-0.131	$\mathrm{TBE^{13}}$
1AP		0.97	0.93	+0.04	\exp^{28a}
$5AP(C_{2v})$		2.128	2.274	-0.147	this work
5AP		2.231	2.365	-0.134	$ADC(2)^9$
5AP		1.971	2.056		
$5AP(C_{2v})$		2.177	2.296	-0.119	$\mathrm{TBE^{13}}$
5AP		1.957	2.003	-0.047	$0-0, \exp^{30}$
					, 1
$7AP (D_{3h})$		2.636	2.889	-0.253	this work
7AP			2.998		$ADC(2)^9$
7AP		2.512			0-0, $ADC(2)^9$
$7AP (D_{3h})$		2.717	2.936	-0.219	$\mathrm{TBE^{13}}$
7AP				<0	\exp^{3}
, , , , ,					0.1.p.
$2AP(C_{2v})$	2.1	0.838	0.941	-0.102	this work
$2AP(C_s)$		1.246	1.121	+0.125	
$2AP(C_{2v})$		0.833	0.904	-0.071	TBE^{13}
2111 (0 ₂ V)		0.000	0.001	0.0.1	122
$3AP(C_{2v})$	5.3	0.689	0.768	-0.079	this work
$3AP(C_s)$	0.0	1.335			this work
$3AP(C_{2v})$		0.693	0.735	-0.042	TBE^{13}
0111 (C2v)		0.000	0.100	0.042	100
$4AP(D_{3h})$	11.1	0.550	0.623	_0.073	this work
$4AP (C_{3h})$	11.1	1.409		+0.392	
$4AP (D_{3h})$		0.554	0.583	-0.029	TBE^{13}
-171 (D3h)		0.004	0.000	-0.029	TDE

 $[^]a$ Using S1=0.78 μm^{-1} and T1=0.75 μm^{-1} from Ref. 28 multiplied by 1.2398 eV/ μm^{-1} .

and 7AP, and found no evidence for symmetry lowering via in-plane distortions. For 5AP and 7AP, STGs calculated with ADC(2)/aug-cc-pVTZ based on geometries determined with CCSD(T)/cc-pVTZ show deviations of about 0.03 eV from TBEs. The structural stability of 5AP and 7AP, confirmed by the CCSD(T)-level analysis, indicates that both molecules violate Hund's rule in their minimum energy geometry with high-symmetry. From previously reported ADC(2)-level vertical and 0-0 values of STG, one can correct the TBE of the vertical STG of 5AP from Ref. 13 to be -0.07 eV, agreeing with the

experimental value of -0.047 eV^{30} . As the precise value of the STG of 7AP is unknown, the TBE values corrected for 0-0 excitation amounts to -0.083 eV, which is lower than -0.011 eV from the fluorescence measurements⁵ of a substituted 7AP.

We found the NICS(1)_{iso} values of 5AP and 7AP to have very small magnitudes, indicating these two systems to be non-aromatic with localized charge density. The other four systems in their symmetric structure exhibit large positive NICS(1)_{iso} values 1 Å above the centroid of their rings indicating anti-aromaticity⁵⁰, for the symmetric geometries determined at the ω B97X-D/ccpVTZ-level, in the order: 1AP < 2AP < 3AP < 4AP (see Figure S4).

To understand whether anti-aromaticity increases the multi-reference character of their ground state, we inspect the T_1 -diagnostic metric, which is the Frobenius norm of the single substitution amplitudes vector (t_1) obtained from the closed-shell CCSD wave function divided by the square root of the number of correlated electrons⁵¹. A magnitude of T_1 less than 0.02 indicates that the ground state is predominantly of a singlereference nature for which the single-reference method, CCSD(T), which we have applied for geometry optimization, is appropriate. For fully optimized structures at the CCSD(T)/cc-pVTZ level, we found the T_1 values to be: $0.017 \text{ (1AP: } D_{3h} \& C_{3h}), 0.017 \text{ (2AP: } C_{2v}), 0.015 \text{ (2AP: } C_{2v})$ $C_{\rm s}$), 0.016 (3AP: $C_{\rm 2v}$), 0.015 (3AP: $C_{\rm s}$), 0.016 (4AP: $D_{3h}~\&~C_{3h}$), indicating single-reference nature. Interestingly, the T_1 values for 5AP (C_{2v}) and 7AP (D_{3h}) were close to the threshold, 0.019 and 0.020, respectively, indicating the need to investigate these systems with multireference methods. Furthermore, as the systems with the small NICS(1)_{iso} values—5AP and 7AP—show larger T_1 values, for azaphenalenes, one can conclude that antiaromaticity does not imply a multi-reference character of the ground state.

C. Jahn-Teller Analysis

We rationalize the symmetry lowering in APs as a vibronically driven process on the basis of the Jahn–Teller (JT) theorem^{52–54}. Specifically, we verify if the symmetry of the vibrational normal mode corresponding to the distortion, as seen in DFT results, agrees with the JT theorem. The electronic ground state energy, $E_0(q)$, is expanded as a truncated Taylor series in the distortion coordinate, q:

$$E_0(q) = E_0 + \langle 0|\hat{H}'|0\rangle q + \frac{1}{2}kq^2,$$
 (1)

where E_0 corresponds to the ground state energy in the undistorted equilibrium geometry (at q=0), and \hat{H}' is the first derivative of the electronic Hamiltonian with respect to q. At q=0, the coefficient in the first-order JT contribution, $\langle 0|\hat{H}'|0\rangle$, vanishes for APs; however, this term can be non-zero for systems with degenerate elec-

tronic states. For pseudo-degenerate (*i.e.*, near degenerate) electronic states, the second-order term in q^2 can be non-zero, where k is the total force constant that includes contributions from vibronic coupling⁵⁵

$$k = \langle 0|\hat{H}''|0\rangle - 2\sum_{n\neq 0} \frac{|\langle 0|\hat{H}'|n\rangle|^2}{E_n - E_0}.$$
 (2)

Here \hat{H}'' is second derivative of the electronic Hamiltonian with respect to q, and E_n is the energy of the n-th electronic state at q = 0.

The second-order term gives rise to the pseudo-JT contribution capable of stabilizing the system upon distortion from q=0, provided there is a low-lying state, n, of correct symmetry such that $\langle 0|\hat{H}'|n\rangle \neq 0$. For this, the product of the corresponding irreducible representations, $\Gamma_0 \times \Gamma_q \times \Gamma_n$, should contain the totally symmetric representation of the point group corresponding to the symmetric structure. If this group is Abelian, then the condition is $\Gamma_q = \Gamma_0 \times \Gamma_n$. For 1AP and 4AP, the totally symmetric irreducible representation is A_1' of D_{3h} , and for 2AP and 3AP, it is A_1 of C_{2v} . We write the irreducible representations in small case alphabets when denoting the MOs and use large cases for the states and vibrational modes.

Assuming that there is only one low-lying excited state, $|1\rangle$, coupling with the ground state, we arrive at

$$k = \langle 0|\hat{H}''|0\rangle - 2\frac{|\langle 0|\hat{H}'|1\rangle|^2}{E_1 - E_0} = k_0 - k_{0,1}.$$
 (3)

Here, $k_0 \geq 0$ is the force constant of the symmetric structure in the absence of vibronic coupling, while the condition for distortion is k < 0. The second term of Eq. 3, $k_{0,1}$, cannot be negative, as it is a ratio of two positive numbers. Hence, symmetry-lowering is prominent when $k_0 < k_{0,1}$, which requires a significantly large $|\langle 0|\hat{H}'|1\rangle|^2$, small $E_1 - E_0$ or both. This explains why symmetry lowering is not observed in 5AP and 7AP with fairly large $S_0 \rightarrow S_1$ excitation energies of about 2.1, and 2.6 eV (see TABLE I). On the other hand, the ADC(2)/cc-pVTZexcitation energy of S_1 is 1.0 eV in 1AP (D_{3h}) , which decreases to 0.8, 0.7, and 0.6 eV in 2AP (C_{2v}) , 3AP (C_{2v}) , and 4AP (D_{3h}) , respectively. Overall, our analysis suggests that inverted-STG candidates with small values of $S_0 \to S_1$ may exhibit strong structural distortions warranting more detailed analysis such as the JTH diagnostics presented in this study.

The symmetry of the ground electronic state of the APs, in their high-symmetry geometry, correspond to the totally symmetric irreducible representations: A_1 of C_{2v} and A_1' of D_{3h} . If the irreducible representation of $|1\rangle$ is non-degenerate, the product of the irreducible representations of \hat{H}' and $|1\rangle$ should be totally symmetric, which is possible only when q and $|1\rangle$ belong to the same irreducible representation. The character of the HOMO and LUMO in all APs are similar, see Figure S3. For

molecules in D_{3h} point group, the symmetries are a_1'' and a_2'' , respectively, while for those in C_{2v} , the symmetries are a_2 and b_1 , respectively. The symmetry of the excited state, $|1\rangle$, when considering a Slater-determinant form, is the product, $\Gamma_{\text{HOMO}} \times \Gamma_{\text{LUMO}}$. Hence, the symmetry of the excited state under concern is A_2' for 1AP and 4AP (in D_{3h}) and B_2 for 2AP and 3AP (in C_{2v}).

In our $\omega B97X$ -D/cc-pVTZ calculations, the wavenumbers of the distortion modes of 2AP, 3AP, and 4AP are $340i \text{ cm}^{-1}$ (B_2), $773i \text{ cm}^{-1}$ (B_2), and $1113i \text{ cm}^{-1}$ (A'_2), respectively; see Table S4 in the SI. The corresponding k (in Eq. 3) are -0.6402, -3.8163, and -8.6171mdyne/Å, respectively. This trend shows how the distortion becomes stronger with increasing N in the electrondeficient sites of 1AP. While we have presented evidence for enhanced distortion with the lowering of $E_1 - E_0$, it is also important to understand the role of the coupling term $|\langle 0|\hat{H}'|1\rangle|^2$. One can heuristically estimate this quantity through two conditions: 1) the expectation value of the second-derivative term is similar in both distorted and undistorted geometries, 2) in the lowsymmetry (i.e., distorted) structure, there is no vibronic coupling. These two conditions amount to

$$k_{\text{high-sym.}} = k_{\text{low-sym.}} - 2 \frac{|\langle 0|\hat{H}'|1\rangle|^2}{E_1 - E_0}.$$
 (4)

The meaning of $|\langle 0|\hat{H}'|1\rangle|$ is the magnitude of force due to vibronic coupling in the high-symmetry structure; this quantity will increase in magnitude, going from 2AP to 3AP to 4AP in the same order as the strength of the distortion. The corresponding $k_{\text{low-sym.}}$ (in Eq. 4), determined using frequency calculations at the minimum energy geometries, are 0.0454, 0.0479, and 0.0522 mdyne/Å, respectively.

Hence, one can determine $|\langle 0|\hat{H}'|1\rangle|$ as

$$|\langle 0|\hat{H}'|1\rangle| = \sqrt{\frac{(k_{\text{low-sym.}} - k_{\text{high-sym.}})(E_1 - E_0)}{2}}. \quad (5)$$

resulting in 1.308, 2.906, and 4.029 eV/Å for 2AP, 3AP, and 4AP, respectively. At the ω B97XD level 1AP does not undergo distortion, hence in Eq. 4, $k_{\rm high-sym.} = k_{\rm low-sym.}$ resulting in $|\langle 0|\hat{H}'|1\rangle| = 0$. The increase in the strength of distortion in the order 2AP<3AP<4AP is a combined effect of decreasing S₁-S₀ gap, and increasing $|\langle 0|\hat{H}'|1\rangle|$ in Eq. 3.

The Jahn–Teller active normal mode corresponds to in-plane stretching, with symmetries A_2' (for $D_{3\mathrm{h}} \to C_{3\mathrm{h}}$ transition) and B_2 (for $C_{2\mathrm{v}} \to C_{\mathrm{s}}$ transition). Upon symmetry lowering, the irreducible representation is A', which is the totally symmetric representation in $C_{3\mathrm{h}}$ and C_{s} . This observation follows the epikernel principle: preferred distortions of JT unstable molecules are directed towards the largest subgroup such that the JT active mode in the subgroup is totally symmetric⁵⁶.

D. Ground and excited state energies of 4AP along Jahn–Teller active normal mode

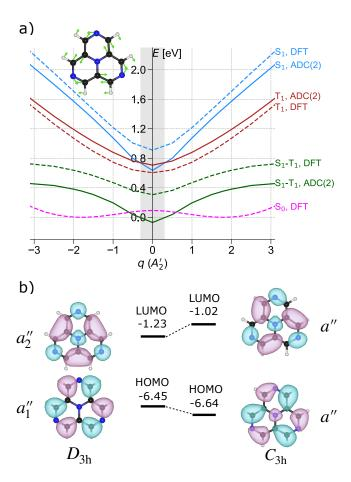


FIG. 5. Pseudo-Jahn-Teller distortion in 4AP according to ω B97X-D/cc-pVTZ modeling: a) Potential energy profile of 4AP along the Jahn-Teller active dimensionless normal coordinate, q, of A'_2 symmetry. The force constant matrix was computed at the D_{3h} geometry (q = 0), a first-order saddle point with an imaginary frequency (1113i cm⁻¹); the inset shows the normal mode. The DFT ground electronic state energy is denoted S₀ (pink, dashed) and the symmetry lowers to C_{3h} when $q \neq 0$. The excited state energies, S_1 (blue), T₁ (red), and singlet-triplet gap, S₁-T₁, (green) determined using ADC(2)/cc-pVTZ and ω B97X-D3/cc-pVTZ methods are represented by bold and dashed lines, respectively. The singlet-triplet gap is negative within the shaded region $-0.3 \le q \le 0.3$ at the ADC(2) level. b) Frontier MOs of 4AP in D_{3h} and C_{3h} structures showing the HOMO-LUMO gap increases due to better symmetry-allowed atomic orbital interactions in the C_{3h} structure.

FIG. 5a shows the ground and excited state energies of 4AP along the JT active mode of the D_{3h} configuration. The S_0 energy was determined at the DFT level, while the excited state energies were calculated using ADC(2) and DFT methods. The S_0 profile shows the doublewell character at the DFT level, whereas, at the same DFT level, the S_1 and T_1 profiles are predicted as sin-

gle wells. The excited state energies also show singlewell character at the ADC(2) level. It is interesting to note that the ground state analogue of ADC(2), MP2, predicts the structure of 4AP to be D_{3h} in disagreement with CCSD(T). The notable difference between predictions of the excited state profiles by both methods is that according to ADC(2), S_1 has lower energy than T_1 at the D_{3h} configuration (q = 0). The ADC(2)level STG remains negative for slight distortions from the D_{3h} structure, while at $q \approx 1.8$ (corresponding to the C_{3h} minimum), the STG increases to +0.344 eV (see Table S4). At the ω B97X-D3 level, with the Tamm-Dancoff approximation, the STG is positive and somewhat uniform for all values of q. Overall, the DFT and ADC(2) profiles shown in FIG. 5a suggest that a method capable of predicting the double-well profile for S_0 does not need to predict the negative sign of the STG and vice versa.

The main driving force for the pseudo-JT effect is the improved orbital interactions permitted by symmetry lowering. Analysis of the HOMO and LUMO plots of 4AP in D_{3h} and C_{3h} configurations reveals that the a_1'' and a_2'' MOS (HOMO and LUMO) transform as a_1'' upon symmetry lowering, see FIG. 5b. A mild splitting of the HOMO-LUMO gap is noted upon distortion, imparting more stability to the ground state. Subsequently, symmetry lowering enhances the exchange interaction between HOMO and LUMO in the C_{3h} structure, resulting in a more stable T_1 state compared to S_1 .

IV. CONCLUSIONS

In conclusion, we conducted a diagnostic analysis followed by full geometry optimizations to determine if the symmetric structures of APs are true minima on the PES and to investigate the dependence of their STG on structural distortions. Out of six APs studied here, the D_{3h} structure of the prototypical molecule, cyclazine (1AP), is predicted to be a saddle point by CCSD(T) with the correct minimum identified to have the C_{3h} symmetry. The mildly anti-aromatic nature of the ring-current in the symmetric form suggests the possibility of symmetry-lowering as in the case of cyclobutadiene in the D_{4h} structure⁵⁰. While cyclobutadiene exhibits a first-order JT effect, in the closed-shell system 1AP the effect stems from second-order interactions. When including high-level and adiabatic corrections, our estimation of the STG of 1AP in the C_{3h} structure explains the experimental value of 0.04 eV^{28} better than the more negative STG of the D_{3h} structure. As the energy difference between the high and low-symmetry structures of 1AP is very small, future works can apply higher-level methods such as CCSDT or CCSDT(Q) for identifying the true minimum of 1AP.

5AP and 7AP with N atoms at electron-rich sites do not show symmetry lowering at the CCSD(T)-level and exhibit negative STG in ADC(2) calculations in line with the experimental results^{3,30} and TBEs¹³. Three APs

with N at the electron-deficient sites—2AP, 3AP, and 4AP—show stronger tendencies for symmetry lowering, even when modeled with a long-range corrected DFT method. While at the correct minima determined with CCSD(T), these molecules show positive STGs, popular methods such as MP2 and B3LYP prefer symmetric structures leading to negative STGs in subsequent excited state modeling, suggesting a violation of Hund's rule. More rigorous studies should be conducted on the sensitivity of STGs to symmetry constraints of inverted-STG candidates not explored in this study. Our calculations show that 4AP exhibits significant pseudo-Jahn-Teller distortions, with the STG at the C_{3h} structure exceeding 0.3 eV, which is above the threshold for efficient thermally-activated-delayed-fluorescence (TADF) emitters with rapid $rISC^{57-59}$. It is essential to ensure that novel properties capable of a paradigm shift in the theoretical understanding of molecules withstand the artifacts of quantum chemistry approximations.

V. SUPPLEMENTARY INFORMATION

i) Tables S1–S4 compare STGs from our calculations to results from past works; ii) Figure S1 presents potential energy surface plots of S_0 calculated with DFT methods; iii) Figure S2 presents potential energy surface plots of S_1 and T_1 calculated with ADC(2); iv) Figure S3 presents plots of HOMO and LUMO; v) Figure S4 presents NICS(1)_{iso} and NICS(1)_{zz} values; vi) Frozencore CCSD(T)/cc-pVTZ equilibrium coordinates and Z-matrix.

VI. DATA AVAILABILITY

The data that support the findings of this study are within the article and its supplementary material.

VII. ACKNOWLEDGMENTS

We acknowledge the support of the Department of Atomic Energy, Government of India, under Project Identification No. RTI 4007. All calculations have been performed using the Helios computer cluster, which is an integral part of the MolDis Big Data facility, TIFR Hyderabad (http://moldis.tifrh.res.in).

VIII. AUTHOR DECLARATIONS

A. Author contributions

AM: Conceptualization (main); Analysis (equal); Data collection (equal); Writing (main). **KJ**: Analysis (equal);

Data collection (equal). **SD**: Analysis (equal); Data collection (equal). **RR**: Conceptualization (main); Analysis (equal); Data collection (equal); Funding acquisition; Project administration and supervision; Resources; Writing (main).

B. Conflicts of Interest

The authors have no conflicts of interest to disclose.

IX. REFERENCES

- ¹W. Kutzelnigg and J. Morgan, Z. Phys. D Atoms Molec. Clusters 36, 197 (1996).
- ²P. de Silva, J. Phys. Chem. Lett. **10**, 5674 (2019).
- ³J. Ehrmaier, E. J. Rabe, S. R. Pristash, K. L. Corp, C. W. Schlenker, A. L. Sobolewski, and W. Domcke, J. Phys. Chem. A 123, 8099 (2019).
- ⁴R. Pollice, P. Friederich, C. Lavigne, G. dos Passos Gomes, and A. Aspuru-Guzik, Matter 4, 1654 (2021).
- ⁵N. Aizawa, Y.-J. Pu, Y. Harabuchi, A. Nihonyanagi, R. Ibuka, H. Inuzuka, B. Dhara, Y. Koyama, K.-i. Nakayama, S. Maeda, et al., Nature 609, 502 (2022).
- ⁶J. Li, Z. Li, H. Liu, H. Gong, J. Zhang, Y. Yao, and Q. Guo, Front. Chem. **10**, 999856 (2022).
- ⁷G. Ricci, J.-C. Sancho-García, and Y. Olivier, J. Mater. Chem. C 10, 12680 (2022).
- ⁸S. Ghosh and K. Bhattacharyya, J. Phys. Chem. A **126**, 1378 (2022).
- ⁹L. Tučková, M. Straka, R. R. Valiev, and D. Sundholm, Phys. Chem. Chem. Phys. 24, 18713 (2022).
- ¹⁰M. Bedogni, D. Giavazzi, F. Di Maiolo, and A. Painelli, J. Chem. Theory Comput. **20**, 902 (2023).
- ¹¹T. Won, K.-i. Nakayama, and N. Aizawa, Chem. Phys. Rev. 4
- ¹²D. Drwal, M. Matousek, P. Golub, A. Tucholska, M. Hapka, J. Brabec, L. Veis, and K. Pernal, J. Chem. Theory Comput. 19, 7606 (2023).
- ¹³P.-F. Loos, F. Lipparini, and D. Jacquemin, J. Phys. Chem. Lett. **14**, 11069 (2023).
- ¹⁴R. Pollice, B. Ding, and A. Aspuru-Guzik, Matter 7, 1161 (2024).
- ¹⁵M. H. Garner, J. T. Blaskovits, and C. Corminboeuf, Chem. Commun. **60**, 2070 (2024).
- ¹⁶D. Valverde, C. T. Ser, G. Ricci, K. Jorner, R. Pollice, A. Aspuru-Guzik, and Y. Olivier, ACS Appl. Mater. Interfaces (2024).
- ¹⁷R. Cunningham, D. Farquhar, W. Gibson, and D. Leaver, J. Chem. Soc. C, 239 (1969).
- ¹⁸R. S. Hosmane, M. A. Rossman, and N. J. Leonard, J. Am. Chem. Soc. **104**, 5497 (1982).
- ¹⁹M. Shahbaz, S. Urano, P. R. LeBreton, M. A. Rossman, R. S. Hosmane, and N. J. Leonard, J. Am. Chem. Soc. **106**, 2805 (1984).
- ²⁰M. A. Rossman, N. J. Leonard, S. Urano, and P. R. LeBreton, J. Am. Chem. Soc. **107**, 3884 (1985).
- ²¹B. M. Gimarc, J. Am. Chem. Soc. **105**, 1979 (1983).
- ²²W. Leupin, D. Magde, G. Persy, and J. Wirz, J. Am. Chem. Soc. **108**, 17 (1986).
- ²³E. Heilbronner and Z.-Z. Yang, Angew. Chem. Int. Ed. **26**, 360 (1987).
- ²⁴J. Terence Blaskovits, M. H. Garner, and C. Corminboeuf, Angew. Chem. Int. Ed. **62**, e202218156 (2023).
- ²⁵O. H. Omar, X. Xie, A. Troisi, and D. Padula, J. Am. Chem. Soc. **145**, 19790 (2023).
- ²⁶E. Meiszter, T. Gazdag, P. J. Mayer, A. Kunfi, T. Holczbauer, M. Sulyok-Eiler, and G. London, J. Org. Chem. 89, 5941 (2024).

- ²⁷A. Majumdar and R. Ramakrishnan, Phys. Chem. Chem. Phys. 26, 14505 (2024).
- ²⁸W. Leupin and J. Wirz, J. Am. Chem. Soc. **102**, 6068 (1980).
- ²⁹P. Karak, P. Manna, A. Banerjee, K. Ruud, and S. Chakrabarti, J. Phys. Chem. Lett. **15**, 7603 (2024).
- ³⁰K. D. Wilson, W. H. Styers, S. A. Wood, R. C. Woods, R. J. McMahon, Z. Liu, Y. Yang, and E. Garand, J. Am. Chem. Soc. **146**, 15688 (2024).
- ³¹Y. Kusakabe, K. Shizu, H. Tanaka, K. Tanaka, and H. Kaji, Appl. Phys. Express 17, 061001 (2024).
- ³²A. Dreuw and M. Hoffmann, Front. Chem. **11** (2023).
- 33 M. Kondo, Chem. Phys. Lett. **804**, 139895 (2022).
- ³⁴J. C. Sancho-Garcia, E. Bremond, G. Ricci, A. Pérez-Jiménez, Y. Olivier, and C. Adamo, J. Chem. Phys. **156** (2022).
- ³⁵P. J. Stephens, F. J. Devlin, C. F. Chabalowski, and M. J. Frisch, J. Chem. Phys. **98**, 11623 (1994).
- ³⁶J.-D. Chai and M. Head-Gordon, Phys. Chem. Chem. Phys. **10**, 6615 (2008).
- ³⁷M. J. Frisch, G. W. Trucks, H. B. Schlegel, G. E. Scuseria, M. A. Robb, J. R. Cheeseman, G. Scalmani, V. Barone, G. A. Petersson, H. Nakatsuji, et al., "Gaussian 16 Revision C.01," (2016).
- ³⁸H. Werner, P. Knowles, G. Knizia, F. Manby, M. Schütz, P. Celani, W. Györffy, D. Kats, T. Korona, R. Lindh, et al., "Molpro, version 2015.1, a package of ab initio programs," (2015).
- ³⁹O. Vahtras, J. Almlöf, and M. Feyereisen, Chem. Phys. Lett. 213, 514 (1993).
- ⁴⁰R. A. Kendall and H. A. Früchtl, Theor. Chim. Acta **97**, 158 (1997).
- ⁴¹A. I. Krylov and P. M. Gill, Wiley Interdiscip. Rev. Comput. Mol. Sci. 3, 317 (2013).
- ⁴²P. v. R. Schleyer, C. Maerker, A. Dransfeld, H. Jiao, and N. J. van Eikema Hommes, J. Am. Chem. Soc. 118, 6317 (1996).

- $^{43}\mathrm{F}.$ Neese, Wiley Interdiscip. Rev. Comput. Mol. Sci. $\mathbf{2},$ 73 (2012).
- ⁴⁴F. Neese, Wiley Interdiscip. Rev. Comput. Mol. Sci. 8, e1327 (2018).
- ⁴⁵G. E. Scuseria and H. F. Schaefer, J. Phys. Chem. **94**, 5552 (1990).
- ⁴⁶Z. Sun and H. F. Schaefer III, J. Org. Chem. **84**, 5548 (2019).
- ⁴⁷S. Senthil, S. Chakraborty, and R. Ramakrishnan, Chem. Sci. 12, 5566 (2021).
- ⁴⁸E. R. Davidson and W. T. Borden, J. Phys. Chem. **87**, 4783 (1983).
- ⁴⁹P. S. Zuev, R. S. Sheridan, T. V. Albu, D. G. Truhlar, D. A. Hrovat, and W. T. Borden, Science **299**, 867 (2003).
- ⁵⁰P. B. Karadakov, J. Phys. Chem. A **112**, 7303 (2008).
- ⁵¹J. Wang, S. Manivasagam, and A. K. Wilson, J. Chem. Theory Comput. **11**, 5865 (2015).
- ⁵²H. A. Jahn and E. Teller, Proc. R. Soc. Lond. A **161**, 220 (1937).
- $^{53}{\rm R.~F.~Bader,~Can.~J.~Chem.~40},~1164~(1962).$
- ⁵⁴R. G. Pearson, Proc. Natl. Acad. Sci. USA **72**, 2104 (1975).
- ⁵⁵T. Nakajima, A. Toyota, and M. Kataoka, J. Am. Chem. Soc. 104, 5610 (1982).
- ⁵⁶A. Ceulemans, D. Beyens, and L. Vanquickenborne, J. Am. Chem. Soc. **106**, 5824 (1984).
- ⁵⁷P. K. Samanta, D. Kim, V. Coropceanu, and J.-L. Brédas, J. Am. Chem. Soc. **139**, 4042 (2017).
- ⁵⁸X.-K. Chen, D. Kim, and J.-L. Brédas, Acc. Chem. Res. **51**, 2215 (2018).
- ⁵⁹F.-M. Xie, P. Wu, S.-J. Zou, Y.-Q. Li, T. Cheng, M. Xie, J.-X. Tang, and X. Zhao, Adv. Electron. Mater. 6, 1900843 (2020).

Supplementary information for:

Influence of Pseudo-Jahn-Teller Activity on the Singlet-Triplet Gap of Azaphenalenes

Atreyee Majumdar, Komal Jindal, Surajit Das, and Raghunathan Ramakrishnan*

Tata Institute of Fundamental Research, Hyderabad 500046, India

E-mail: ramakrishnan@tifrh.res.in

Table S1: **Results for 1AP:** Energies of the S_1 and T_1 states with respect to the S_0 ground state along with the singlet-triplet gap, S_1 - T_1 , are given in eV. Methods used for determining the equilibrium geometries and their point groups are also stated. The barrier for automerization, E^{\ddagger} , determined with the method used for optimization is stated in kJ/mol. Results from other studies are included for comparison.

Geometry			Excited states				Source
Method	Symmetry	E^{\ddagger}	Method	S_1	T_1	S_1 - T_1	
B3LYP	$D_{3\mathrm{h}}$, $C_{3\mathrm{h}}$	0.0	ADC(2)	1.004	1.146	-0.143	this work
$\omega \mathrm{B}97\mathrm{X}\text{-}\mathrm{D}$	$D_{3\mathrm{h}},C_{3\mathrm{h}}$	0.0	II.	1.027	1.166	-0.139	II .
MP2	$D_{3\mathrm{h}},C_{3\mathrm{h}}$	0.0	II .	0.997	1.138	-0.141	II .
CCSD	$D_{3\mathrm{h}}$	3.6	II.	1.012	1.153	-0.142	II .
II	$C_{3\mathrm{h}}$		II .	1.391	1.334	+0.057	II .
CCSD(T)	$D_{3\mathrm{h}}$	0.5	II	0.988	1.134	-0.146	II .
II	$C_{3\mathrm{h}}$		II	1.143	1.204	-0.061	II .
B97-3C			NEVPT2(12,12)	1.244	1.288	-0.044	Ref. 1
			RMS-CASPT2	0.89	0.97	-0.08	Ref. 2
MP2			CC2	1.047	1.180	-0.133	Ref. 3
MP2,ADC(2)			CC2(adiabatic)	0.976	1.117	-0.141	Ref. 3
MP2,ADC(2)			CC2 (0-0)	0.992	1.068	-0.076	Ref. 3
$\omega \mathrm{B}97\mathrm{X}\text{-}\mathrm{D}$			EOM-CCSD			-0.072	Ref. 4
CCSD(T)	$D_{3\mathrm{h}}$		ADC(2)	1.001	1.138	-0.137	Ref. 5
CCSD(T)	$D_{3\mathrm{h}}$		ADC(3)	0.81	0.87	-0.06	Ref. 5
CCSD(T)	$D_{3\mathrm{h}}$		TBE	0.979	1.110	-0.131	Ref. 5
exp.			exp.	0.97	0.93	+0.04	Ref. 6^a

^a Using $S_1 = 0.78 \ \mu m^{-1}$ and $T_1 = 0.75 \ \mu m^{-1}$ from Ref. 6 multiplied by 1.2398 eV/ μm^{-1} .

Table S2: **Results for 5AP:** Energies of the S_1 and T_1 states with respect to the S_0 ground state along with the singlet-triplet gap, S_1 - T_1 , are given in eV. Methods used for determining the equilibrium geometries and their point groups are also stated. The barrier for automerization, E^{\ddagger} , determined with the method used for optimization is stated in kJ/mol. Results from other studies are included for comparison.

Geometry			Excited states				Source
Method	Symmetry	E^{\ddagger}	Method	S_1	T_1	S_1 - T_1	
B3LYP	$C_{ m 2v}$, $C_{ m s}$	0.0	ADC(2)	2.129	2.275	-0.146	this work
$\omega \mathrm{B}97\mathrm{X}\text{-}\mathrm{D}$	$C_{ m 2v},C_{ m s}$	0.0	II	2.167	2.307	-0.140	"
MP2	$C_{ m 2v}$		II	2.143	2.288	-0.145	"
CCSD	$C_{ m 2v}$		11	2.161	2.303	-0.142	"
CCSD(T)	$C_{ m 2v}$		11	2.123	2.273	-0.150	"
B97-3C			NEVPT2(8,8)	2.26	2.35	-0.089	Ref. 1
B97-3C			NEVPT2(10,10)			+0.034	Ref. 1
B97-3C			NEVPT2(12,12)			+0.036	Ref. 1
			RMS-CASPT2	2.00	2.08	-0.08	Ref. 2
MP2			CC2	2.231	2.365	-0.134	Ref. 3
MP2, ADC(2)			CC2 (adiabatic)	2.066	2.197	-0.131	Ref. 3
MP2, ADC(2)			CC2 (0-0)	1.971	2.056	-0.085	Ref. 3
$\omega \mathrm{B}97\mathrm{X}\text{-}\mathrm{D}$			EOM-CCSD	2.359	2.397	-0.08	Ref. 7
CCSD(T)	$C_{ m 2v}$		ADC(2)	2.159	2.298	-0.139	Ref. 5
CCSD(T)	$C_{ m 2v}$		TBE	2.177	2.296	-0.119	Ref. 5
exp.			exp.	1.957	2.003	-0.047	Ref. 8

Table S3: **Results for 7AP:** Energies of the S_1 and T_1 states with respect to the S_0 ground state along with the singlet-triplet gap, S_1 - T_1 , are given in eV. Methods used for determining the equilibrium geometries and their point groups are also stated. The barrier for automerization, E^{\ddagger} , determined with the method used for optimization is stated in kJ/mol. Results from other studies are included for comparison.

Geometry			Excited states				Source
Method	Symmetry	E^{\ddagger}	Method	S_1	T_1	S_1 - T_1	
B3LYP	D_{3h} , C_{3h}	0.0	ADC(2)	2.643	2.892	-0.249	this work
$\omega \mathrm{B}97\mathrm{X}\text{-}\mathrm{D}$	$D_{3\mathrm{h}},C_{3\mathrm{h}}$	0.0	II.	2.681	2.925	-0.244	"
MP2	$D_{3\mathrm{h}}$		II .	2.649	2.900	-0.251	11
CCSD	$D_{3\mathrm{h}}$		II	2.670	2.918	-0.249	II .
CCSD(T)	$D_{3\mathrm{h}}$		II	2.626	2.882	-0.256	11
B97-3C			NEVPT2(12,12)	3.259	3.398	-0.139	Ref. 1
			RMS-CASPT2	2.50	2.70	-0.20	Ref. 2
MP2			CC2	2.756	2.998	-0.242	Ref. 3
MP2, ADC(2)			CC2 (adiabatic)	2.640	2.894	-0.254	Ref. 3
MP2, ADC(2)			CC2 (0-0)	2.512	2.618	-0.106	Ref. 3
$\omega \mathrm{B}97\mathrm{X}\text{-}\mathrm{D}$			EOM-CCSD			-0.144	Ref. 4
CCSD(T)	$D_{3\mathrm{h}}$		ADC(2)	2.675	2.927	-0.246	Ref. 5
CCSD(T)	$D_{3\mathrm{h}}$		ADC(3)	2.81	2.88	-0.07	Ref. 5
CCSD(T)	$D_{3\mathrm{h}}$		TBE	2.717	2.936	-0.219	Ref. 5
exp.			exp.			<0	Ref. 9

Table S4: Results for 2AP, 3AP, and 4AP: Energies of the S_1 and T_1 states with respect to the S_0 ground state along with the singlet-triplet gap, S_1 - T_1 , are given in eV. Methods used for determining the equilibrium geometries and their point groups are also stated. The barrier for automerization, E^{\ddagger} , determined with the method used for optimization is stated in kJ/mol. Results from other studies are included for comparison.

Geometry			Excited states				Source
Method	Symmetry	E^{\ddagger}	Method	S_1	T_1	S_1 - T_1	
Results for	or 2AP						
B3LYP	$C_{ m 2v},C_{ m s}$	0.0	ADC(2)	0.872	0.975	-0.103	this work
$\omega \mathrm{B}97\mathrm{X}\text{-}\mathrm{D}$	$C_{2v}(B_2, 340i \text{ cm}^{-1})$	0.1	II	0.894	0.993	-0.099	"
"	$C_{ m s}$		II .	1.007	1.041	-0.034	"
MP2	$C_{ m 2v}$	0.3	II	0.861	0.960	-0.099	"
"	$C_{ m s}$		II .	0.851	0.948	-0.097	"
CCSD	$C_{ m 2v}$	9.6	II	0.885	0.988	-0.102	"
"	$C_{ m s}$		II .	1.481	1.269	+0.212	"
CCSD(T)	$C_{ m 2v}$	2.5	II .	0.856	0.962	-0.106	"
"	$C_{ m s}$		II .	1.269	1.145	+0.125	"
B97-3C			NEVPT2(12,12)			-0.120	Ref. 1
			RMS-CASPT2	0.89	0.97	-0.08	Ref. 2
CCSD(T)	$C_{ m 2v}$		ADC(2)	1.001	1.138	-0.137	Ref. 5
CCSD(T)	$C_{ m 2v}$		TBE	0.833	0.904	-0.071	Ref. 5
Results fo	or 3AP						
B3LYP	$C_{ m 2v}$, $C_{ m s}$	0.0	ADC(2)	0.743	0.827	-0.084	this work
$\omega \mathrm{B}97\mathrm{X}\text{-}\mathrm{D}$	$C_{2v}(B_2, 773i \text{ cm}^{-1})$	1.9	II	0.765	0.845	-0.079	II .
11	$C_{ m s}$		II	1.238	1.049	+0.189	II .
MP2	$C_{ m 2v}$, $C_{ m s}$		II	0.711	0.790	-0.079	II .
CCSD	$C_{ m 2v}$	16.8	II	0.745	0.826	-0.081	II .
11	$C_{ m s}$		II	1.555	1.225	+0.330	II .
CCSD(T)	$C_{ m 2v}$	5.9	II	0.714	0.797	-0.083	II .
11	$C_{ m s}$		II	1.367	1.093	+0.274	II .
CCSD(T)	$C_{ m 2v}$		ADC(2)	2.159	2.298	-0.139	Ref. 5
CCSD(T)	$C_{ m 2v}$		TBE	0.693	0.735	-0.042	Ref. 5
Results for							
B3LYP	$D_{3h}(A_2', 494i \text{ cm}^{-1}))$	0.2	ADC(2)	0.614	0.689	-0.075	this work
11	$C_{3\mathrm{h}}$		II	0.916	0.791	+0.125	11
$\omega \mathrm{B}97\mathrm{X}\text{-}\mathrm{D}$	$D_{3h}(A_2', 1113i \text{ cm}^{-1})$	5.5	II	0.636	0.707	-0.071	11
11	$C_{3\mathrm{h}}$		II	1.377	1.033	+0.344	11
MP2	$D_{3\mathrm{h}}$, $C_{3\mathrm{h}}$		II	0.573	0.648	-0.074	11
CCSD	$D_{3 m h}$	26.3	II	0.614	0.688	-0.073	11
11	$C_{3\mathrm{h}}$		II	1.635	1.203	+0.432	11
CCSD(T)	$D_{3\mathrm{h}}$	11.6	II	0.582	0.660	-0.078	II .
"	$C_{3\mathrm{h}}$		II	1.452	1.057	+0.395	II .
CCSD(T)	$D_{3\mathrm{h}}$		ADC(2)	2.675	2.927	-0.246	Ref. 5
CCSD(T)	$D_{3\mathrm{h}}$		TBE	0.554	0.583	-0.029	Ref. 5

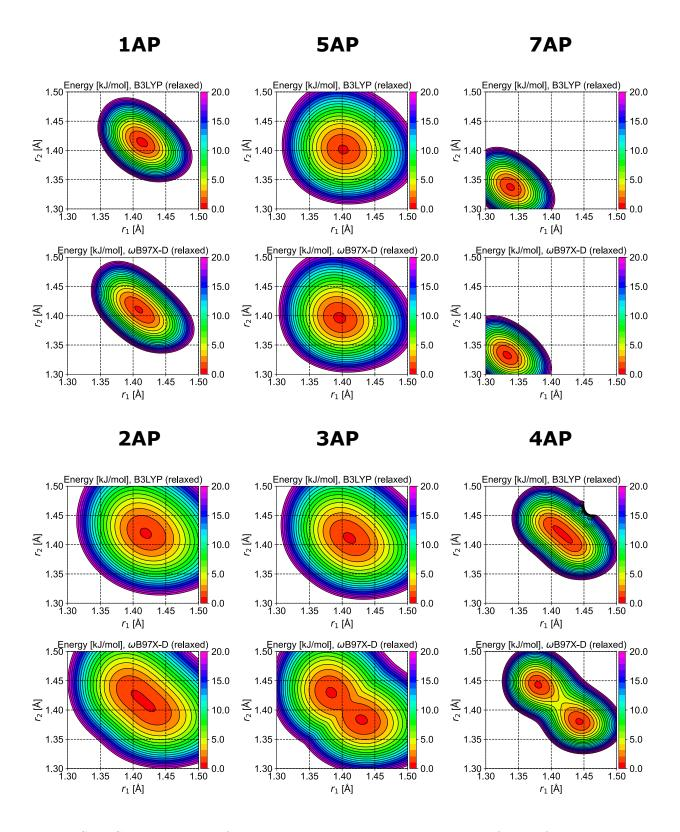


Figure S1: Contour plots of two-dimensional potential energy surfaces of azaphenalenes calculated with the DFT methods: B3LYP and ω B97X-D. See the main text for more details.

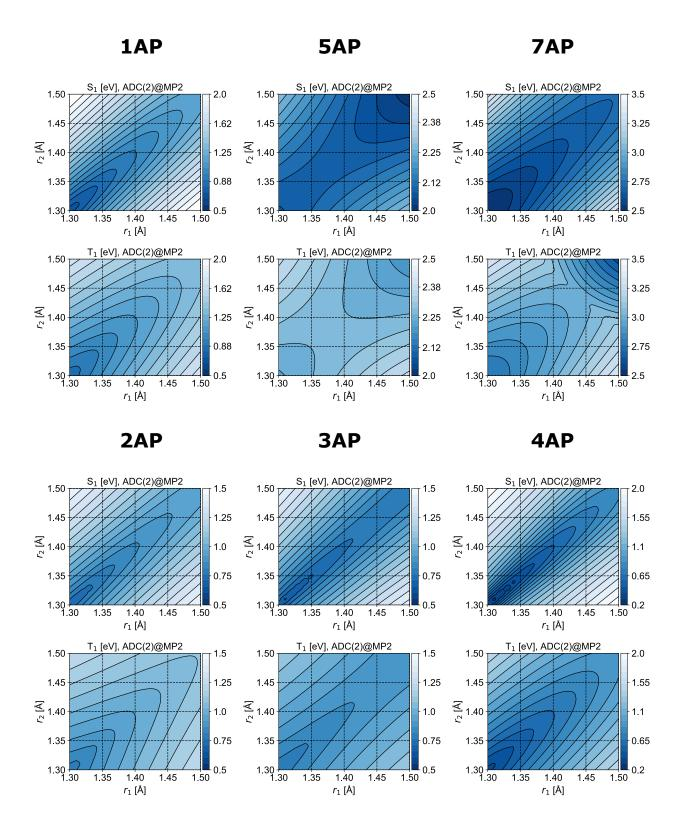


Figure S2: Contour plots of S_1 and T_1 energies of azaphenalenes. See the main text for more details.

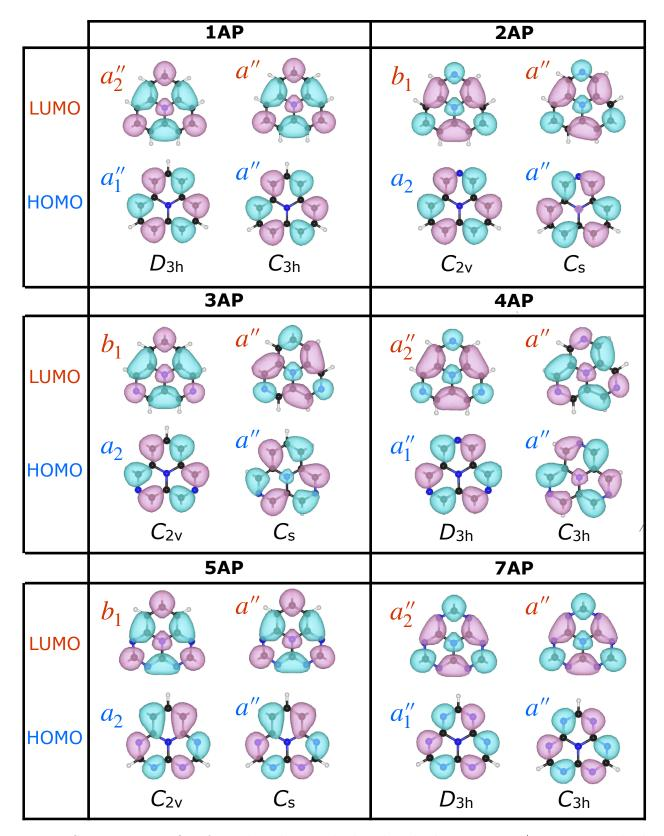


Figure S3: Frontier MOs of azaphenalenes calculated with the ω B97X-D/cc-pVTZ method in the respective equilibrium geometries.

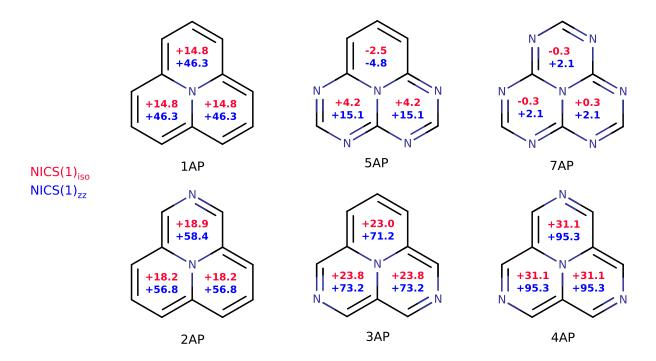


Figure S4: Nucleus-independent chemical shifts (NICS) calculated with the ω B97X-D3/cc-pVTZ method.

EQUILIBRIUM COORDINATES (ANGSTROEM), FROZEN-CORE CCSD(T)/cc-pVTZ MOLECULE: 1AP, POINT GROUP: D3H

CARTESIAN COORDINATES

22

22			
CCSD(T)/CC-PVTZ ENERGY=-51	6.45718151	
N	-0.000000000	0.000000000	0.000000000
С	1.4090613106	0.000000000	0.000000000
С	-0.7045306553	-1.2202828904	0.000000000
С	-0.7045306553	1.2202828904	0.000000000
С	2.0972867575	-1.2322296003	0.000000000
С	-2.1157855159	-1.2001888109	0.000000000
C	0.0184987584	2.4324184112	0.000000000
C	1.4038057208	-2.4314628324	0.000000000
C	-2.8076114416	0.000000000	0.000000000
C	1.4038057208	2.4314628324	0.000000000
C	0.0184987584	-2.4324184112	0.000000000
С	-2.1157855159	1.2001888109	0.000000000
С	2.0972867575	1.2322296003	0.000000000
H	3.1771396445	-1.1950402229	0.000000000
H	-2.6235050138	-2.1539635320	0.000000000
H	-0.5536346307	3.3490037549	0.000000000
H	1.9455458220	-3.3697842121	0.000000000
H	-3.8910916439	0.000000000	0.000000000
H	1.9455458220	3.3697842121	0.000000000
H	-0.5536346307	-3.3490037549	0.000000000
H	-2.6235050138	2.1539635320	0.000000000
H	3.1771396445	1.1950402229	0.000000000

Z-MATRIX

geometry={ N1, R1 C1 , N1 , R1 , C1 , 120.0 C2 , N1 , R1 , C1 , 120.0 , C2 , 180.0 C3 , N1 C4 , C1 , R2 , N1 , A1 , C3 , 180.0, C2 , R2 , N1 , A1 , C1 , 180.0 C5 , C2 , 180.0 , C3 C6 , R2 , N1 , A1 , R3 , C1 , 60.0 , C4 , 0.0 C7 , N1 C8 , N1 , R3 , C2 , 60.0 , C5 , 0.0 C9 , N1 , R3 , C3 , 60.0 , C6 , 0.0 C10 , C2 , R2 , N1 , A1 , C3 , 180.0

```
\mbox{H13} , \mbox{C4} , \mbox{R4} , \mbox{C1} , \mbox{A2} , \mbox{N1} , \mbox{180.0}
H14 , C5
          , R4 , C2 , A2
                               , N1 , 180.0
H15 , C6
           , R4 , C3 , A2
                                   N1 , 180.0
H16 , N1
           , R5 , C1
                      , 60.0
                               , C4 , 0.0
   , N1
                               , C5 , 0.0
H17
          , R5 , C2 , 60.0
   , N1
           , R5 , C3
                      , 60.0
                               , C6 , 0.0
H18
                               , N1 , 180.0
H19 , C10 , R4 ,
                    C2 , A2
                               , N1 , 180.0
H2O , C11 , R4 , C3 , A2
H21 , C12 , R4 , C1 , A2 , N1 , 180.0}
R1= 1.40906131
                ANG
R2= 1.41139791
                ANG
R3= 2.80761144
                ANG
R4= 1.08049309
                ANG
R5= 3.89109164
                ANG
A1= 119.18425212 DEGREE
A2= 117.21180516 DEGREE
```

11

EQUILIBRIUM COORDINATES (ANGSTROEM), FROZEN-CORE CCSD(T)/cc-pVTZ MOLECULE: 1AP, POINT GROUP: C3H

CARTESIAN COORDINATES

22

22			
CCSD(T)	CC-PVTZ ENERGY=-516	6.45737101	
N	-0.000000000	-0.000000000	0.000000000
C	1.4102958789	0.000000000	0.000000000
C	-0.7051479395	-1.2213520580	0.000000000
C	-0.7051479395	1.2213520580	0.000000000
C	2.0874818807	-1.2604285404	0.000000000
C	-2.1353040760	-1.1775980685	0.000000000
C	0.0478221953	2.4380266088	0.000000000
C	1.3925819281	-2.4404907466	0.000000000
C	-2.8098179483	0.0142340467	0.000000000
C	1.4172360202	2.4262566999	0.000000000
C	-0.0118165536	-2.4277621932	0.000000000
C	-2.0965954569	1.2241145322	0.000000000
C	2.1084120105	1.2036476610	0.000000000
H	3.1682050232	-1.2317091765	0.000000000
H	-2.6507939485	-2.1278914463	0.000000000
H	-0.5174110747	3.3596006228	0.000000000
H	1.9254527231	-3.3837087737	0.000000000
H	-3.8931041186	0.0243634149	0.000000000
H	1.9676513955	3.3593453588	0.000000000
H	-0.5905645004	-3.3398001629	0.000000000
H	-2.5970695345	2.1813439414	0.000000000
Н	3.1876340349	1.1584562216	0.000000000

Z-MATRIX

geometry={ N1, R1 C1 , N1 C2 , N1 , R1 , C1 , 120.0 , N1 , R1 , C1 , 120.0 , C2 , 180.0 C3 C4 , C1 , R21 , N1 , A11 , C3 , 180.0 , C2 , R21 , N1 , A11 , C1 , 180.0 C5 , C3 , R21 , N1 , A11 , C2 , 180.0 C6 , R3 , C1 , A3 , C4 , 0.0 C7 , N1 C8 , N1 , R3 , C2 , A3 , C5 , 0.0 C9 , N1 , R3 , C3 , A3 , C6 , 0.0 C10 , C2 , R22 , N1 , A12 , C3 , 180.0 $\mathtt{C11}$, $\mathtt{C3}$, $\mathtt{R22}$, $\mathtt{N1}$, $\mathtt{A12}$, $\mathtt{C1}$, $\mathtt{180.0}$ C12 , C1 , R22 , N1 , A12 , C2 , 180.0

```
H13 , C4
            , R41 ,
                      C1 , A21
                                    , N1 , 180.0
H14
       C5
              R41
                      C2
                          , A21
                                          , 180.0
                                      N1
H15
       C6
               R41
                      C3
                             A21
                                      N1
                                             180.0
    , N1
                                         , 0.0
H16
              R5
                      C1
                                      C4
                            A4
                      C2 ,
H17
    , N1
              R5
                            A4
                                      C5
                                             0.0
    , N1
                                         , 0.0
H18
              R5
                      C3
                             A4
                                      C6
H19
       C10
                      C2 ,
                             A22
               R42
                                      N1 , 180.0
H20
    , C11
               R42
                      СЗ
                             A22
                                      N1
                                         , 180.0
    , C12
                      C1 ,
H21
              R42
                             A22
                                      N1 ,
                                             180.0}
R1=
     1.41029588
                   ANG
R21= 1.43082528
                   ANG
R22= 1.39145026
                   ANG
R3=
     2.80985400
                   ANG
R41= 1.08110467
                   ANG
R42= 1.08016779
                   ANG
R5=
     3.89318035
                   ANG
A11= 118.24764782
                  DEGREE
A12= 120.11375054
                   DEGREE
A21= 116.72541599
                   DEGREE
A22= 117.71594276
                   DEGREE
A3=
     60.29024792
                   DEGREE
A4=
     60.35855774
                   DEGREE
```

13

EQUILIBRIUM COORDINATES (ANGSTROEM), FROZEN-CORE CCSD(T)/cc-pVTZ MOLECULE: 5AP, POINT GROUP: C2V

CARTESIAN COORDINATES

18

18			
CCSD(T)/	CC-PVTZ ENERGY=-58	30.61455705	
N	0.000000000	0.000000000	-0.0209337139
C	0.000000000	0.000000000	1.3959162652
C	0.000000000	1.2239982977	-0.6919457558
C	0.000000000	-1.2239982977	-0.6919457558
C	0.000000000	1.2095528292	-2.0899593840
C	0.000000000	-1.2095528292	-2.0899593840
C	0.000000000	0.000000000	-2.7748568006
N	0.000000000	2.3932182796	-0.0052415583
N	0.000000000	-2.3932182796	-0.0052415583
C	0.000000000	2.2752712648	1.3127808253
C	0.000000000	-2.2752712648	1.3127808253
N	0.000000000	-1.1592137265	2.0571477735
N	0.000000000	1.1592137265	2.0571477735
H	0.000000000	2.1667462052	-2.5888851619
H	0.000000000	-2.1667462052	-2.5888851619
H	0.000000000	0.000000000	-3.8578325493
H	0.000000000	3.2048943207	1.8718610719
H	0.000000000	-3.2048943207	1.8718610719

Z-MATRIX

geometry={

Q1 N2 , Q1 , 1.0 C3 , N2 , R1 ,Q1 , 90.0 , R2 ,C3 , N2 , A1 , Q1 , 90.0 C4 C5 , N2 , R2 ,C3 , A1 , Q1 , -90.0 , C4 C6 , R3 ,N2 , A2 , C3 , 180.0 , C5 , R3 , C3 , 180.0 C7 ,N2 , A2 , R4 ,Q1 , N2 C8 , 90.0 , C3 , 180.0 , C4 , R5 ,C6 , A3 , C8 , 180.0 N9 N10 , C5 , R5 ,C7 , A3 , C8 , 180.0 , R6 ,C4 C11 , N9 , A4 , C6 , 180.0 , C7 , 180.0 C12 , N10 , R6 ,C5 , A4 , R7 N13 , C3 ,N2 , A5 , Q1 , 90.0 N14 , C3 , R7 ,N2 , A5 , Q1 , -90.0 H15 , C6 , R8 ,C4 , A6 , N2 , 180.0 , R8 H16 , C7 ,C5 , A6 , N2 , 180.0

H17 , N2 , R9 ,Q1 , 90.0 , C3 , 180.0

```
, C4 , 180.0
H18 , C11 , R10 ,N9 , A7
H19
    , C12 , R10 ,N10 , A7 , C5 , 180.0}
R1=
     1.41684998
                   ANG
R2=
     1.39586138
                   ANG
R3=
     1.39808826
                   ANG
     2.75392309
                   ANG
R4=
R5=
     1.35596387
                   ANG
     1.32328927
R6=
                   ANG
R7=
     1.33454246
                   ANG
R8=
     1.07941933
                   ANG
     3.83689884
R9=
                   ANG
R10=
     1.08479019
                   ANG
A1=
     118.73213541
                   DEGREE
A2=
     118.14012765
                   DEGREE
     121.01850011
                   DEGREE
A3=
A4=
     115.31283627
                   DEGREE
A5=
     119.70103198
                   DEGREE
     116.93824030
                   DEGREE
A6=
A7=
     115.90926862 DEGREE
```

EQUILIBRIUM COORDINATES (ANGSTROEM), FROZEN-CORE CCSD(T)/cc-pVTZ MOLECULE: 7AP, POINT GROUP: D3H

CARTESIAN COORDINATES

16			
CCSD(T)/CC-PVTZ ENERGY=-61:	2.67978274	
N	-0.000000000	0.000000000	0.000000000
C	1.4025590960	0.000000000	0.000000000
C	-0.7012795480	-1.2146518075	0.000000000
C	-0.7012795480	1.2146518075	0.000000000
N	2.0624112763	-1.1624036292	0.000000000
N	-2.0378767105	-1.2048987437	0.000000000
N	-0.0245345658	2.3673023730	0.000000000
C	1.3055871332	-2.2613432484	0.000000000
C	-2.6111742664	0.000000000	0.000000000
C	1.3055871332	2.2613432484	0.000000000
N	-0.0245345658	-2.3673023730	0.000000000
N	-2.0378767105	1.2048987437	0.000000000
N	2.0624112763	1.1624036292	0.000000000
H	1.8477262446	-3.2003557341	0.000000000
H	-3.6954524892	0.000000000	0.000000000
H	1.8477262446	3.2003557341	0.000000000

Z-MATRIX _____

```
geometry={
```

C1 , N1 , R1

N1

C2 , N1 , R1 , C1 , 120.0

C3 , N1 , R1 , C1 , 120.0 , C2 , 180.0 ${\tt N4}$, ${\tt C1}$, ${\tt R2}$, ${\tt N1}$, ${\tt A1}$, ${\tt C3}$, ${\tt 180.0}$, C1 , 180.0 N5 , C2 , R2 , N1 , A1 N6 , C3 , R2 , N1 , A1 , C2 , 180.0 C7 , N1 , R3 , C1 , 60.0 , N4 , 0.0 C8 , N1 , R3 , C2 , 60.0 , N5 , 0.0 , N1 , R3 , C3 , 60.0 , N6 , 0.0 C9 N10 , C2 , R2 , N1 , A1 , C3 , 180.0 , C1 , 180.0 N11 , C3 , R2 , N1 , A1 $\mbox{N12}$, $\mbox{C1}$, $\mbox{R2}$, $\mbox{N1}$, $\mbox{A1}$, $\mbox{C2}$, $\mbox{180.0}$ $\rm H16$, $\rm N1$, $\rm R4$, $\rm C1$, $\rm 60.0$, $\rm N4$, $\rm 0.0$

H17 , N1 , R4 , C2 , 60.0 , N5 , 0.0 $\,$ H18 , N1 , R4 , C3 , 60.0 , N6 , 0.0}

R1= 1.40255910 ANG R2= 1.33663275 ANG R3= 2.61117427 ANG R4= 3.69545249 ANG A1= 119.58192379 DEGREE

EQUILIBRIUM COORDINATES (ANGSTROEM), FROZEN-CORE CCSD(T)/cc-pVTZ MOLECULE: 2AP, POINT GROUP: C2V

CARTESIAN COORDINATES

21			
CCSD(T))/CC-PVTZ ENERGY=-53	32.47959209	
N	0.000000000	0.000000000	0.0248325005
C	0.000000000	0.000000000	1.4290623782
C	0.000000000	1.2078318281	-0.6816722169
C	0.000000000	-1.2078318281	-0.6816722169
C	0.000000000	1.1361626851	-2.0998624488
C	0.000000000	-1.1361626851	-2.0998624488
N	0.000000000	0.000000000	-2.7913610218
C	0.000000000	2.4312143725	0.0133915849
C	0.000000000	-2.4312143725	0.0133915849
C	0.000000000	2.4361423616	1.4014105437
C	0.000000000	-2.4361423616	1.4014105437
C	0.000000000	-1.2409740228	2.1053260238
C	0.000000000	1.2409740228	2.1053260238
H	0.000000000	2.0691835901	-2.6488864922
H	0.000000000	-2.0691835901	-2.6488864922
H	0.000000000	3.3405675958	-0.5697082153
H	0.000000000	-3.3405675958	-0.5697082153
H	0.000000000	3.3764935994	1.9393551417
H	0.000000000	-3.3764935994	1.9393551417
H	0.000000000	-1.2161284987	3.1855901804
Н	0.000000000	1.2161284987	3.1855901804

Z-MATRIX

```
geometry={
Q1
             , 1.0
N2 , Q1
   , N2
C3
           , R1 , Q1 , 90.0
            , R21 , C3 , A11 , Q1 , 90.0
C4 , N2
   , N2
C5
           , R21 , C3 , A11 , Q1 , -90.0
{\tt C6} , {\tt C4} , {\tt 1.42} , {\tt N2} , {\tt A21} , {\tt C3} , {\tt 180.0}
\mbox{C7} , \mbox{C5} , \mbox{1.42} , \mbox{N2} , \mbox{A21} , \mbox{C3} , \mbox{180.0}
           , R4
                    , Q1
N8 , N2
                            , 90.0 , C3 , 180.0
C9 , C4 , R51 , C6 , A31 , N8 , 180.0
\texttt{C10} , \texttt{C5} , \texttt{R51} , \texttt{C7} , \texttt{A31} , \texttt{N8} , \texttt{180.0}
C11 , C9
            , R61 , C4 , A41 , C6 , 180.0
C12 , C10 , R61 , C5 , A41 , C7 , 180.0
\text{C13} , \text{C3} , \text{R71} , \text{N2} , \text{A51} , \text{Q1} , 90.0
C14 , C3 , R71 , N2 , A51 , Q1 , -90.0
```

```
, C4
    , C6
             , R81
                              , A61
H15
                                      , N2 , 180.0
H16
       C7
                     , C5
               R81
                                 A61
                                         N2
                                                 180.0
H17
       C9
               R91
                         C4
                                 A71
                                          N2
                                                 180.0
     , C10
                        C5
H18
               R91
                                 A71
                                         N2
                                                180.0
H19
      C11 ,
               R101
                         C9
                              , A81
                                          C4
                                                 180.0
H20
       C12
               R101
                         C10
                                 A81
                                          C5
                                                180.0
H21
       C13
               R111
                         СЗ
                                 A91
                                          N2
                                                 180.0
H22
       C14 ,
               R111
                         СЗ
                                          N2
                                                 180.0}
                                 A91
R1=
       1.40422988
                     ANG
                     ANG
R21=
       1.39928790
R4=
       2.81619352
                     ANG
R51=
       1.40704603
                    ANG
R61=
       1.38802771
                    ANG
R71=
       1.41327600
                    ANG
R81=
       1.08256889
                     ANG
                     ANG
R91=
       1.08024472
R101=
       1.08334890
                     ANG
                     ANG
R111=
       1.08054984
A11=
       120.32491617
                    DEGREE
A21=
                    DEGREE
       117.43189871
A31=
       122.49605497
                     DEGREE
A41=
       119.80645820
                    DEGREE
A51=
       118.58799201
                     DEGREE
A61=
       117.58111363
                     DEGREE
A71=
       117.72796459
                     DEGREE
       119.97590106
A81=
                    DEGREE
A91=
       117.27045062 DEGREE
```

19

EQUILIBRIUM COORDINATES (ANGSTROEM), FROZEN-CORE CCSD(T)/cc-pVTZ MOLECULE: 2AP, POINT GROUP: CS

CARTESIAN COORDINATES

21			
CCSD(T)/C	C-PVTZ ENERGY=-5	32.48054565	
N	0.000000000	-0.0045831784	0.0256744030
C	0.000000000	-0.0653222374	1.4328110801
C	0.000000000	1.2349703896	-0.6238470103
C	0.000000000	-1.1796125221	-0.7439882171
C	0.000000000	1.2001927918	-2.0721810380
C	0.000000000	-1.0755525634	-2.1230678573
N	0.000000000	0.1172406921	-2.7966089725
C	0.000000000	2.4209431626	0.0784696912
C	0.000000000	-2.4422851071	-0.0575750796
C	0.000000000	2.3859073808	1.4986888985
C	0.000000000	-2.4928065436	1.3058067208
C	0.000000000	-1.2937083640	2.0669099437
C	0.000000000	1.1868583471	2.1491593335
H	0.000000000	2.1601623484	-2.5787913104
H	0.000000000	-1.9796425986	-2.7154936531
H	0.000000000	3.3481710306	-0.4755702300
H	0.000000000	-3.3337207740	-0.6698562121
H	0.000000000	3.3094589364	2.0645423722
H	0.000000000	-3.4495452735	1.8138331151
H	0.000000000	-1.3101702046	3.1471666469
Н	0.000000000	1.1246713808	3.2292659990

Z-MATRIX

geometry={ Q1 , 1.0 N2 , Q1 , N2 , R1 , Q1 , 90.0 C3 C4 , N2 , R21 , C3 , A11 , Q1 , 90.0C5 , N2 , R22 , C3 , A12 , Q1 , -90.0C6 , C4 , R31 , N2 , A21 , C3 , 180.0 $\mbox{C7}$, $\mbox{C5}$, $\mbox{R32}$, $\mbox{N2}$, $\mbox{A22}$, $\mbox{C3}$, $\mbox{180.0}$ N8 , N2 , R4 , Q1 , 90.0 , C3 , 180.0 C9 , C4 , R51 , C6 , A31 , N8 , 180.0 C1O , C5 , R52 , C7 , A32 , N8 , 180.0C11 , C9 , R61 , C4 , A41 , C6 , 180.0 C12 , C10 , R62 , C5 , A42 , C7 , 180.0 C13 , C3 , R71 , N2 , A51 , Q1 , 90.0C14 , C3 , R72 , N2 , A52 , Q1 , -90.0

```
H15
        C6
                 R81
                           C4
                                    A61
                                              N2
                                                      180.0
H16
        C7
                 R82
                           C5
                                    A62
                                              N2
                                                      180.0
H17
        C9
                 R91
                           C4
                                    A71
                                              N2
                                                      180.0
H18
                 R92
                           C5
        C10
                                    A72
                                              N2
                                                      180.0
H19
        C11
                 R101
                           C9
                                    A81
                                              C4
                                                      0.08
H20
        C12
                 R102
                           C10
                                    A82
                                                      180.0
                                              C5
H21
        C13
                 R111
                           СЗ
                                    A91
                                              N2
                                                      180.0
H22
                           СЗ
                                                      180.0}
        C14
                 R112
                                    A92
                                              N2
R1=
       1.40844697
                       ANG
R21=
                       ANG
       1.39941813
R22=
       1.40466171
                       ANG
R31=
       1.44875151
                       ANG
R32=
       1.38300005
                       ANG
R4=
       2.82491142
                       ANG
R51=
       1.37832513
                       ANG
                       ANG
R52=
       1.43718651
R61=
       1.42065130
                       ANG
R62=
       1.36431754
                       ANG
R71=
       1.38239424
                       ANG
R72=
                       ANG
       1.44260564
R81=
       1.08544715
                       ANG
R82=
       1.08090107
                       ANG
R91=
                       ANG
       1.08014432
R92=
       1.08145538
                       ANG
R101=
       1.08311478
                       ANG
R102=
       1.08325427
                       ANG
R111=
       1.08038213
                       ANG
R112=
       1.08189539
                       ANG
A11=
       120.12600781
                       DEGREE
A12=
       120.75378845
                       DEGREE
A21=
       116.27883973
                       DEGREE
A22=
       118.91028829
                       DEGREE
A31=
       122.00896152
                       DEGREE
A32=
       122.84449320
                       DEGREE
A41=
       119.22027278
                       DEGREE
A42=
       120.65153460
                       DEGREE
A51=
       119.77464009
                       DEGREE
A52=
       117.30139889
                       DEGREE
A61=
       116.44668394
                       DEGREE
A62=
       118.92060510
                       DEGREE
A71=
       118.50728259
                       DEGREE
A72=
       116.98748256
                       DEGREE
A81=
       120.08234665
                      DEGREE
A82=
       120.09039442
                       DEGREE
A91=
       118.17605456
                       DEGREE
A92=
       116.47787965
                      DEGREE
```

EQUILIBRIUM COORDINATES (ANGSTROEM), FROZEN-CORE CCSD(T)/cc-pVTZ MOLECULE: 3AP, POINT GROUP: C2V

CARTESIAN COORDINATES

20

20			
CCSD	(T)/CC-PVTZ ENERGY=-548	3.50029036	
N	0.000000000	0.000000000	-0.0290948978
C	0.000000000	0.000000000	1.3669984084
C	-1.2168465284	0.000000000	-0.7084797812
C	1.2168465284	0.000000000	-0.7084797812
C	-1.2064367713	0.000000000	-2.1185246596
C	1.2064367713	0.000000000	-2.1185246596
C	0.000000000	0.000000000	-2.8062433640
C	-2.4039234215	0.000000000	0.0664921221
C	2.4039234215	0.000000000	0.0664921221
N	-2.4222905439	0.000000000	1.3968479847
N	2.4222905439	0.000000000	1.3968479847
C	1.2485138341	0.000000000	2.0294160803
C	-1.2485138341	0.000000000	2.0294160803
H	-2.1584950794	0.000000000	-2.6293185356
H	2.1584950794	0.000000000	-2.6293185356
H	0.000000000	0.000000000	-3.8894859148
H	-3.3500423056	0.000000000	-0.4592347960
H	3.3500423056	0.000000000	-0.4592347960
Н	1.2501853399	0.000000000	3.1116676060
Н	-1.2501853399	0.000000000	3.1116676060

Z-MATRIX

geometry={

Q1

 $\mbox{N2}$, $\mbox{Q1}$, 1. $\mbox{C3}$, $\mbox{N2}$, $\mbox{R1}$, $\mbox{Q1}$, 90.

C6 , C4 , R31 , N2 , A21 , C3 , 180. C7 , C5 , R31 , N2 , A21 , C3 , 180.

 $\mbox{C8}$, $\mbox{N2}$, $\mbox{R4}$, $\mbox{Q1}$, $\mbox{90.}$, $\mbox{C3}$, $\mbox{180.}$

C9 , C4 , R51 , C6 , A31 , C8 , 180. C10 , C5 , R51 , C7 , A31 , C8 , 180.

N11 , C9 , R61 , C4 , A41 , C6 , 180.

N12 , C10 , R61 , C5 , A41 , C7 , 180. C13 , C3 , R71 , N2 , A51 , Q1 , 90.

C14 , C3 , R71 , N2 , A51 , Q1 , -90.

H15 , C6 , R81 , C4 , A61 , N2 , 180.

```
, R81
H16 , C7
                   , C5 , A61 , N2 , 180.
H17
     , N2
                       Q1
                               90.,
                                       СЗ
               R9
                                              180.
H18
       C9
               R101
                        C4
                               A71
                                       N2
                                              180.
H19
       C10
               R101
                     , C5
                               A71
                                       N2
                                              180.
H20
       C13 , R111
                        СЗ
                               A81 ,
                                       N2
                                             180.
H21
    , C14 , R111 , C3
                            , A81 ,
                                       N2 , 180.}
                    ANG
R1=
       1.39609331
                    ANG
R21=
       1.39365681
R31=
       1.41008330
                    ANG
R4=
      2.77714847
                    ANG
R51=
       1.41765052
                    ANG
R61=
      1.33048265
                    ANG
R71=
                    ANG
       1.41335911
R81=
       1.08042834
                    ANG
R9=
       3.86039102
                    ANG
                    ANG
R101=
      1.08237227
R111=
      1.08225282
                    ANG
       119.17532185 DEGREE
A11=
A21=
       118.75233935
                    DEGREE
A31=
       123.56111295
                    DEGREE
A41=
       123.92911561
                    DEGREE
A51=
       117.94885423
                    DEGREE
A61=
       117.79125752
                    DEGREE
A71=
       117.80239208
                    DEGREE
A81=
       118.03734581 DEGREE
```

24

EQUILIBRIUM COORDINATES (ANGSTROEM), FROZEN-CORE CCSD(T)/cc-pVTZ MOLECULE: 3AP, POINT GROUP: CS

CARTESIAN COORDINATES

20

CCSD(T)/	CC-PVTZ ENERGY=-548.	50254805				
N N	-0.0301087996	0.000000000	-0.0071919123			
=-						
C	1.3672653196	0.000000000	0.0434018915			
C	-0.7451386686	0.000000000	1.1985859497			
C	-0.6743830266	0.000000000	-1.2451826933			
C	-2.1854701157	0.000000000	1.1008388321			
C	-2.0478183588	0.000000000	-1.3162538802			
C	-2.8111683861	0.000000000	-0.1078839037			
C	-0.0667671869	0.000000000	2.3955584988			
C	0.1946360907	0.000000000	-2.4104311060			
N	1.3092378138	0.000000000	2.4841624359			
N	1.4945797827	0.000000000	-2.3753924311			
C	2.0868659377	0.000000000	-1.1279470207			
C	1.9703973364	0.000000000	1.3638484277			
H	-2.7395722113	0.000000000	2.0300723981			
H	-2.5188281841	0.000000000	-2.2885833186			
H	-3.8933635152	0.000000000	-0.1470662294			
H	-0.6238735158	0.000000000	3.3211015155			
H	-0.2953113948	0.000000000	-3.3792420842			
H	3.1668701502	0.000000000	-1.0931161855			
H	3.0551323907	0.000000000	1.4020293484			

Z-MATRIX

geometry={

Q1

N2 , Q1 , 1.

C3 , N2 , R1 , Q1 , 90. C4 , N2 , R21 , C3 , A11 , Q1 , 90.

 ${\tt C5}$, ${\tt N2}$, ${\tt R22}$, ${\tt C3}$, ${\tt A12}$, ${\tt Q1}$, ${\tt -90}.$

C6 , C4 , R31 , N2 , A21 , C3 , 180. C7 , C5 , R32 , N2 , A22 , C3 , 180.

C8 , N2 , R4 , Q1 , 90. , C3 , 180. C9 , C4 , R51 , C6 , A31 , C8 , 180.

C10 , C5 , R52 , C7 , A32 , C8 , 180.

N11 , C9 , R61 , C4 , A41 , C6 , 180.

N12 , C10 , R62 , C5 , A42 , C7 , 180. C13 , C3 , R71 , N2 , A51 , Q1 , 90.

C14 , C3 , R72 , N2 , A52 , Q1 , -90.

H15 , C6 , R81 , C4 , A61 , N2 , 180.

```
, C7
              , R82
                       , C5
                              , A62 ,
H16
                                          N2
                                                 180.
                                          СЗ
H17
        N2
                R9
                          Q1
                                 90.
                                                 180.
H18
        C9
                R101
                          C4
                                 A71
                                          N2
                                                 180.
H19
        C10
                R102
                          C5
                                 A72
                                          N2
                                                 180.
H20
        C13
                R111
                          СЗ
                                 A81
                                          N2
                                                 180.
H21
        C14
                R112
                          C3
                                 A82 ,
                                          N2
                                                180.}
R1=
       1.39828973
                      ANG
R21=
       1.40184449
                      ANG
R22=
                      ANG
       1.39560397
R31=
       1.44364441
                      ANG
R32=
       1.37527296
                      ANG
R4=
       2.78288183
                      ANG
R51=
       1.37583834
                      ANG
R52=
       1.45361552
                      ANG
R61=
       1.37885475
                      ANG
R62=
       1.30041582
                      ANG
R71=
       1.37473027
                      ANG
R72 =
       1.45167052
                      ANG
R81=
       1.08189840
                      ANG
R82=
       1.08040492
                      ANG
R9=
       3.86578605
                      ANG
       1.08027651
                      ANG
R101=
R102=
       1.08565337
                      ANG
                      ANG
R111=
       1.08056573
R112=
       1.08540680
                      ANG
       118.59450254
A11=
                      DEGREE
A12=
                      DEGREE
       119.56690131
A21=
       116.78568095
                      DEGREE
A22=
       120.45558028
                     DEGREE
A31=
       123.42432210
                      DEGREE
A32=
       123.75260069
                      DEGREE
A41=
       123.22624833
                      DEGREE
A42=
       125.17086814
                      DEGREE
A51=
       119.49029669
                      DEGREE
A52=
       116.62276352
                      DEGREE
A61=
       116.92524294
                      DEGREE
A62=
       118.80843317
                      DEGREE
A71=
       119.41333011
                      DEGREE
A72=
       116.45850051
                      DEGREE
A81=
       119.71667571
                      DEGREE
A82=
       116.56508535 DEGREE
```

EQUILIBRIUM COORDINATES (ANGSTROEM), FROZEN-CORE CCSD(T)/cc-pVTZ MOLECULE: 4AP, POINT GROUP: D3H

CARTESIAN COORDINATES

19

10			
CCSD	(T)/CC-PVTZ ENERGY=-564	.51919933	
N	-0.000000000	0.000000000	0.000000000
C	1.3895222367	0.000000000	0.000000000
C	-0.6947611183	-1.2033615561	0.000000000
C	-0.6947611183	1.2033615561	0.000000000
C	2.0427788439	-1.2553814140	0.000000000
C	-2.1085816179	-1.1414076661	0.000000000
C	0.0658027740	2.3967890801	0.000000000
N	1.3980302792	-2.4214594740	0.000000000
N	-2.7960605583	0.000000000	0.000000000
N	1.3980302792	2.4214594740	0.000000000
C	0.0658027740	-2.3967890801	0.000000000
C	-2.1085816179	1.1414076661	0.000000000
C	2.0427788439	1.2553814140	0.000000000
H	3.1249114130	-1.2687198584	0.000000000
H	-2.6611993341	-2.0718927391	0.000000000
H	-0.4637120789	3.3406125974	0.000000000
H	-0.4637120789	-3.3406125974	0.000000000
H	-2.6611993341	2.0718927391	0.000000000
H	3.1249114130	1.2687198584	0.000000000

Z-MATRIX

geometry={

N1												
C1	,	N1	,	R1								
C2	,	N1	,	R1	,	C1	,	120.0				
C3	,	N1	,	R1	,	C1	,	120.0	,	C2	,	180.0
C4	,	C1	,	R2	,	N1	,	A11	,	C3	,	180.0
C5	,	C2	,	R2	,	N1	,	A11	,	C1	,	180.0
C6	,	СЗ	,	R2	,	N1	,	A11	,	C2	,	180.0
N2	,	N1	,	R3	,	C1	,	60.0	,	C4	,	0.0
NЗ	,	N1	,	R3	,	C2	,	60.0	,	C5	,	0.0
N4	,	N1	,	R3	,	C3	,	60.0	,	C6	,	0.0
C7	,	C2	,	R2	,	N1	,	A11	,	СЗ	,	180.0
C8	,	СЗ	,	R2	,	N1	,	A11	,	C1	,	180.0
C9	,	C1	,	R2	,	N1	,	A11	,	C2	,	180.0
H1	,	C4	,	R41	,	C1	,	A21	,	N1	,	180.0
H2	,	C5	,	R41	,	C2	,	A21	,	N1	,	180.0
НЗ	,	C6	,	R41	,	C3	,	A21	,	N1	,	180.0

```
H4 , C7 , R41 , C2 , A21 , N1 , 180.0

H5 , C8 , R41 , C3 , A21 , N1 , 180.0

H6 , C9 , R41 , C1 , A21 , N1 , 180.0}

R1= 1.38952224 ANG

R2= 1.41517726 ANG

R3= 2.79606056 ANG

R41= 1.08221477 ANG

A11= 117.49089295 DEGREE

A21= 118.19708911 DEGREE
```

EQUILIBRIUM COORDINATES (ANGSTROEM), FROZEN-CORE CCSD(T)/cc-pVTZ MOLECULE: 4AP, POINT GROUP: C3H

CARTESIAN COORDINATES

19

19								
CCSD(T)/CC-PVTZ ENERGY=-564.52363202								
N	-0.000000000	0.000000000	0.000000000					
C	1.3943168701	0.000000000	0.000000000					
C	-0.6971584351	-1.2075138304	0.000000000					
C	-0.6971584351	1.2075138304	0.000000000					
C	2.0196953303	-1.3136437071	0.000000000					
C	-2.1474964870	-1.0922856104	0.000000000					
C	0.1278011567	2.4059293175	0.000000000					
N	1.3797047458	-2.4440919420	0.000000000					
N	-2.8064980839	0.0271866114	0.000000000					
N	1.4267933381	2.4169053306	0.000000000					
C	-0.0029504215	-2.3888647060	0.000000000					
C	-2.0673423109	1.1969874930	0.000000000					
C	2.0702927324	1.1918772130	0.000000000					
H	3.1047933775	-1.3373701978	0.000000000					
H	-2.7105932543	-2.0201448396	0.000000000					
H	-0.3942001232	3.3575150373	0.000000000					
H	-0.5363847240	-3.3282397792	0.000000000					
H	-2.6141478367	2.1286426868	0.000000000					
H	3.1505325607	1.1995970924	0.000000000					

Z-MATRIX

geometry={

N1C1 , N1 , R1 C2 , N1 , R1 , C1 , 120.0 $\mbox{C3}$, $\mbox{N1}$, $\mbox{R1}$, $\mbox{C1}$, $\mbox{120.0}$, $\mbox{C2}$, $\mbox{180.0}$ C4 , C1 , R21 , N1 , A11 , C3 , 180.0C5 , C2 , R21 , N1 , A11 , C1 , 180.0C6 , C3 , R21 , N1 , A11 , C2 , 180.0 , C4 , 0.0 N2 , N1 , R3 , C1 , A3 , C5 , 0.0 N3 , N1 , R3 , C2 , A3 N4 , N1 , R3 , C3 , A3 , C6 , 0.0 , C3 , 180.0 C7 , C2 , R22 , N1 , A12 C8 , C3 , R22 , N1 , A12 , C1 , 180.0 $\mbox{C9}$, $\mbox{C1}$, $\mbox{R22}$, $\mbox{N1}$, $\mbox{A12}$, $\mbox{C2}$, $\mbox{180.0}$ H1 , C4 , R41 , C1 , A21 , N1 , 180.0 $\mbox{H2}$, $\mbox{C5}$, $\mbox{R41}$, $\mbox{C2}$, $\mbox{A21}$, $\mbox{N1}$, $\mbox{180.0}$

H3 , C6 , R41 , C3 , A21 , N1 , 180.0

```
\rm H4 , \rm C7 , \rm R42 , \rm C2 , \rm A22 , \rm N1 , \rm 180.0
\mbox{H5} , \mbox{C8} , \mbox{R42} , \mbox{C3} , \mbox{A22} , \mbox{N1} , \mbox{180.0}
H6 , C9 , R42 , C1 , A22 , N1 , 180.0}
R1= 1.39431687
                   ANG
R21= 1.45490825
                   ANG
R22= 1.37022431
                  ANG
R3= 2.80662976
                 ANG
R41= 1.08535742
                    ANG
R42= 1.08026741
                    ANG
A11= 115.45743707 DEGREE
A12= 119.55983802 DEGREE
A21= 116.71005308 DEGREE
A22= 119.96929245 DEGREE
A3= 60.55500817
                    DEGREE
```

References

- (1) Ricci, G.; San-Fabián, E.; Olivier, Y.; Sancho-García, J.-C. Singlet-triplet excited-state inversion in heptazine and related molecules: assessment of TD-DFT and ab initio methods. *ChemPhysChem* **2021**, *22*, 553–560.
- (2) Valverde, D.; Ser, C. T.; Ricci, G.; Jorner, K.; Pollice, R.; Aspuru-Guzik, A.; Olivier, Y. Computational Investigations of the Detailed Mechanism of Reverse Intersystem Crossing in Inverted Singlet-Triplet Gap Molecules. *ACS Appl. Mater. Interfaces* **2024**,
- (3) Tučková, L.; Straka, M.; Valiev, R. R.; Sundholm, D. On the origin of the inverted singlet—triplet gap of the 5th generation light-emitting molecules. *Phys. Chem. Chem. Phys* **2022**, *24*, 18713–18721.
- (4) Garner, M. H.; Blaskovits, J. T.; Corminboeuf, C. Double-bond delocalization in non-alternant hydrocarbons induces inverted singlet-triplet gaps. *Chemical Science* **2023**, *14*, 10458–10466.
- (5) Loos, P.-F.; Lipparini, F.; Jacquemin, D. Heptazine, Cyclazine, and Related Compounds: Chemically-Accurate Estimates of the Inverted Singlet-Triplet Gap. J. Phys. Chem. Lett. 2023, 14, 11069–11075.
- (6) Leupin, W.; Wirz, J. Low-lying electronically excited states of cycl [3.3, 3] azine, a bridged 12. pi.-perimeter. J. Am. Chem. Soc. 1980, 102, 6068–6075.
- (7) Terence Blaskovits, J.; Garner, M. H.; Corminboeuf, C. Symmetry-Induced Singlet-Triplet Inversions in Non-Alternant Hydrocarbons. *Angew. Chem. Int. Ed.* **2023**, *62*, e202218156.
- (8) Wilson, K. D.; Styers, W. H.; Wood, S. A.; Woods, R. C.; McMahon, R. J.; Liu, Z.; Yang, Y.; Garand, E. Spectroscopic Quantification of the Inverted Singlet-Triplet Gap in Pentaazaphenalene. J. Am. Chem. Soc. 2024, 146, 15688–15692.
- (9) Ehrmaier, J.; Rabe, E. J.; Pristash, S. R.; Corp, K. L.; Schlenker, C. W.; Sobolewski, A. L.; Domcke, W. Singlet-triplet inversion in heptazine and in polymeric carbon nitrides. J. Phys. Chem. A 2019, 123, 8099–8108.